

AD-A134 867

CALIBRATION RELATIONSHIPS FOR OPTICALLY MEASURING THE  
CONCENTRATIONS OF B. (U) AIR FORCE WRIGHT AERONAUTICAL  
LABS WRIGHT-PATTERSON AFB OH J J ROME SEP 83

1/1

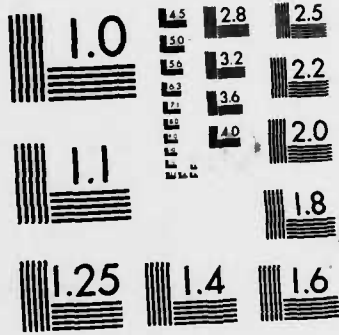
UNCLASSIFIED

AFWAL-TR-83-4051

F/G 20/12

NL





MICROCOPY RESOLUTION TEST CHART  
NATIONAL BUREAU OF STANDARDS-1963-A

10

AD-A134867



CALIBRATION RELATIONSHIPS FOR OPTICALLY MEASURING THE CONCENTRATIONS OF BORON, GALLIUM, AND INDIUM IN SILICON.

John J. Rome

Laser & Optical Materials Branch  
Electromagnetic Materials Division

September 1983

Interim Technical Report for Period July 1982 - December 1982

Approved for Public Release; Distribution Unlimited

DTIC FILE COPY

MATERIALS LABORATORY  
AIR FORCE WRIGHT AERONAUTICAL LABORATORIES  
AIR FORCE SYSTEMS COMMAND  
WRIGHT-PATTERSON AIR FORCE BASE, OHIO 45433

DTIC  
ELECTE  
NOV 21 1983  
S E D

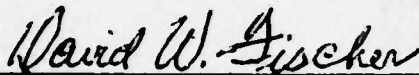
83 11 21 015

NOTICE

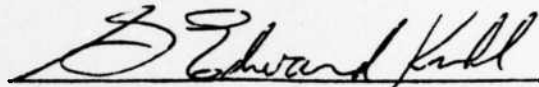
When Government drawings, specifications, or other data are used for any purpose other than in connection with a definitely related Government procurement operation, the United States Government thereby incurs no responsibility nor any obligation whatsoever; and the fact that the government may have formulated, furnished, or in any way supplied the said drawings, specifications, or other data, is not to be regarded by implication or otherwise as in any manner licensing the holder or any other person or corporation, or conveying any rights or permission to manufacture use, or sell any patented invention that may in any way be related thereto.

This report has been reviewed by the Office of Public Affairs (ASD/PA) and is releasable to the National Technical Information Service (NTIS). At NTIS, it will be available to the general public, including foreign nations.

This technical report has been reviewed and is approved for publication.

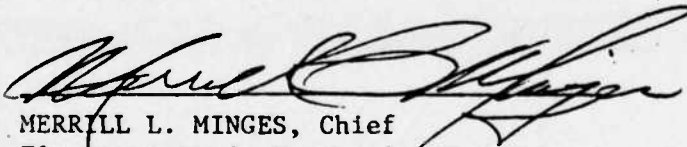


DAVID W. FISCHER  
Project Monitor  
Laser & Optical Materials Branch



G. EDWARD KUHL, Chief  
Laser & Optical Materials Branch  
Electromagnetic Materials Division

FOR THE COMMANDER



MERRILL L. MINGES, Chief  
Electromagnetic Materials Division  
Materials Laboratory  
Air Force Wright Aeronautical Laboratories

"If your address has changed, if you wish to be removed from our mailing list, or if the addressee is no longer employed by your organization please notify AFWAL/MLPO, W-PAFB, OH 45433 to help us maintain a current mailing list".

Copies of this report should not be returned unless return is required by security considerations, contractual obligations, or notice on a specific document.

REPORT DOCUMENTATION PAGE		READ INSTRUCTIONS BEFORE COMPLETING FORM
1. REPORT NUMBER AFWAL-TR-83-4051	2. GOVT ACCESSION NO. AD-A134867	3. RECIPIENT'S CATALOG NUMBER
4. TITLE (and Subtitle) CALIBRATION RELATIONSHIPS FOR OPTICALLY MEASURING THE CONCENTRATIONS OF BORON, GALLIUM, AND INDIUM IN SILICON		5. TYPE OF REPORT & PERIOD COVERED Interim Technical Report July 1982 - December 1982
		6. PERFORMING ORG. REPORT NUMBER
7. AUTHOR(s)  John J. Rome		8. CONTRACT OR GRANT NUMBER(s)
9. PERFORMING ORGANIZATION NAME AND ADDRESS Materials Laboratory (AFWAL/MLPO) Air Force Wright Aeronautical Laboratories, AFSC Wright-Patterson AFB, OH 45433		10. PROGRAM ELEMENT, PROJECT, TASK AREA & WORK UNIT NUMBERS Program Element 61102F Project 2306 TASK 2306Q1 Work Unit 2306Q106
11. CONTROLLING OFFICE NAME AND ADDRESS Materials Laboratory (AFWAL/MLP) Air Force Wright Aeronautical Laboratories, AFSC Wright-Patterson AFB OH 45433		12. REPORT DATE September 1983
		13. NUMBER OF PAGES 69
14. MONITORING AGENCY NAME & ADDRESS (if different from Controlling Office)		15. SECURITY CLASS. (of this report)  Unclassified
		15a. DECLASSIFICATION/DOWNGRADING SCHEDULE
16. DISTRIBUTION STATEMENT (of this Report)  Approved for public release; distribution unlimited.		
17. DISTRIBUTION STATEMENT (of the abstract entered in Block 20, if different from Report)		
18. SUPPLEMENTARY NOTES		
19. KEY WORDS (Continue on reverse side if necessary and identify by block number)  Silicon, infrared absorption, absorption spectra, excitation spectra, fourier transform spectroscopy.		
20. ABSTRACT (Continue on reverse side if necessary and identify by block number) → New, more effective calibration relationships have been experimentally determined which enable FTIR absorption spectroscopy to accurately measure the impurity concentration of In, Ga, and B in silicon. The peak areas of the Group III acceptor related spectra are shown to behave linearly with concen- tration 1/3 or concentration 2/3, rather than simply being proportional to →		

UNCLASSIFIED

SECURITY CLASSIFICATION OF THIS PAGE(When Data Entered)

concentration as was previously assumed. These calibration relationships were determined for optical measurements made on samples cooled to 5K for In and Ga, and 5-8K for B. The relationships for some lines of Ga and In were tested and found to still be accurate for sample temperatures up to 9K. From the high resolution optical measurements made in this study, previously unobserved acceptor related spectral lines were seen. These lines were observed in the  $p_{3/2}$  spectra of In, Ga, Al, and B. Also a  $5p'$  was observed in the  $p_{1/2}$  spectra of Ga. A feature in each acceptor's  $p_{3/2}$  spectrum is defined as  $E_I$ , the ground state binding energy, and the spin-orbit splitting of the silicon valence bands was measured. All the IR induced excited states of In, Ga, Al, and B were measured. After renumbering of the B lines 5 - 11, a more complete correspondence between all the Group III excited state lines was shown than any published previously. ←

UNCLASSIFIED

SECURITY CLASSIFICATION OF THIS PAGE(When Data Entered)

## FOREWORD

This report describes a study performed by the author in partial fulfillment of the requirements for the Master of Science degree in Graduate Engineering Physics at the Air Force Institute of Technology. It was conducted in conjunction with personnel of the Laser and Optical Materials Branch, Electromagnetic Materials Division, Air Force Wright Aeronautical Laboratories, Wright-Patterson Air Force Base, Ohio 45433 under Project No. 2306, Task No. 2306Q1, Work Unit 2306Q106. The report covers work performed during the period July 1982 to December 1982.

I would like to extend my appreciation to the AFWAL Materials Laboratory who funded this project and to those people who supported this study. Special thanks go to Mr. David Fischer who provided stimulating guidance and valuable insight throughout this study. I am grateful to my advisors Mr. David Fischer, Dr. Robert Hengehold, and Dr. Patrick Hemenger whose participation added immeasurably to the success of this research. I would like to thank Dr. William Mitchel, Dr. Patrick Hemenger, Mr. Ken Beasley and Mr. Timothy Peterson for their expertise in the Hall analysis position of this study. Also, to Dr. Michael Glasscock from the University of Missouri Research Reactor facility, I would like to express my thanks for the neutron activation analysis. I am also indebted to Miss Betty Ciani for her assistance in sample selection and to Mr. Robert Burtke for sample preparation. I appreciate the cooperation of those, too numerous to mention here, who provided samples used in this study.

Accession For	
NTIS GRA&I	<input checked="" type="checkbox"/>
DTIC TAB	<input type="checkbox"/>
Unannounced	<input type="checkbox"/>
Justification	
By _____	
Distribution/	
Availability Codes	
Dist	Avail and/or Special
A-1	





## TABLE OF CONTENTS

SECTION	PAGE
I. INTRODUCTION	1
1. Background	1
2. Problem	4
3. Approach	4
4. Scope	5
5. Assumptions	6
II. IR ABSORPTION SPECTRA OF GROUP III ACCEPTORS IN SILICON USED FOR MAKING QUANTITATIVE MEASUREMENTS	7
1. Introduction	7
2. Group III Acceptor IR Spectra	7
3. Using Spectral Lines to Make Quantitative Measurements	10
4. Problems with Previous Calibration Factors	12
III. EXPERIMENTAL EQUIPMENT, MATERIALS, AND PROCEDURE	17
1. Introduction	17
2. Equipment	17
3. Materials	19
4. FTIR Absorption Spectroscopy	20
5. Hall-effect Analysis	23
6. Neutron Activation Analysis	24
IV. EXPERIMENTAL RESULTS AND DISCUSSION	25
1. Introduction	25
2. Absorption Spectra	25
3. Calibration Relationships	30
V. CONCLUSIONS AND RECOMMENDATIONS	41
APPENDIX    ADDITIONAL STRUCTURE IN INFRARED EXCITATION SPECTRA OF GROUP III ACCEPTORS IN SILICON	43
REFERENCES	60



## LIST OF ILLUSTRATIONS

FIGURE		PAGE
1	Photoionization Absorption of Group III - Doped Silicon	2
2	Comparison of Acceptor Spectra In, Ga, Al, and B	8
3	Band Diagram of Acceptor Transitions in Silicon	9
4	Transmittance Spectra of Ga and Al Doped into Silicon	14
5	Temperature Dependence of the Boron $p_{1/2}$ Lines	16
6	Modified Sample Compartment and Isolation Table	18
7	Sample Holders Used for Different Cooling Systems	22
8	IR Absorption Spectrum of Indium-Doped Silicon	26
9	IR Absorption Spectrum of Gallium-Doped Silicon	27
10	IR Absorption Spectrum of Aluminum-Doped Silicon	28
11	IR Absorption Spectrum of Boron-Doped Silicon	29
12	Indium Line 2 Peak Area Versus (a) Concentration, and (b) Concentration <sup>1/3</sup>	31
13	Indium Lines 1,3, and 2p' Peak Area Versus (a) Concentration and (b) Concentration <sup>1/3</sup>	34
14	Boron Lines 1,3,5,2p', and 3p' Peak Area Versus (a) Concentration and (b) Concentration <sup>1/3</sup>	35
15	Gallium Lines 1 and 2p' Peak Area Versus (a) Concentration and (b) Concentration <sup>2/3</sup>	36
16	Gallium Lines 3,5,3p', and 4p' Peak Area Versus (a) Concentration and (b) Concentration <sup>1/3</sup>	37
17	Oxygen Thermometry Curve	40
A-1	$p_{1/2}$ Series Absorption Spectra of Group III Acceptors in Silicon	52
A-2	$p_{3/2}$ Series Absorption Spectrum of Gallium in Silicon	53
A-3	High Energy Region of $p_{3/2}$ Absorption Spectra of Group III Acceptors in Silicon	54
A-4	High Energy Region of $p_{3/2}$ Absorption Spectrum of Boron in Silicon	55
A-5	Experimental Binding Energies of Excited States of Group III Acceptors in Silicon.	56

## LIST OF TABLES

TABLE		PAGE
1	Optical Calibration Constants at 8K (Reference 4)	13
2	Information on Samples Used in this Study	21
3	Optical Calibration Relationships for Boron, Gallium, and Indium in Silicon	32
4	Concentration levels reported by Hall Analysis and Neutron Activation Analysis	38
A-1	$p_{1/2}$ Series Ionization Energy and Some Experimental Energy Separations in Silicon	57
A-2	Experimental Energy Positions of Group III Acceptor Excitation Lines in Silicon	58
A-3	$p_{3/2}$ Ground State Ionization Energies of Group III Acceptors in Silicon	59

## SECTION I

## INTRODUCTION

## 1. BACKGROUND

The Air Force Wright Aeronautical Laboratories (AFWAL) Materials Laboratory is presently conducting research on silicon crystals under Work Unit Directive (WUD) #2306Q106. The purpose of this research is to investigate the electrical and optical properties of silicon materials intended for use in advanced infrared (IR) detector systems and for use in improved electronic devices. In order to understand the optical and electrical behavior of silicon materials, it is extremely helpful to know certain characteristics of the particular sample being studied. Characteristics of special importance, which constitute the subject of this report, are impurity presence and impurity concentration in silicon. It is these impurities which ultimately define the operating limitations of an IR detector or electronic device. For example, it is shown in Figure 1 that by doping different Group III impurities into silicon, one can adjust the optical cutoff frequency of the silicon material, and therefore the cutoff of the IR detector.

Many different techniques are available for studying semiconductor materials and several have been selected for use at the AFWAL Materials Laboratory for thorough electrical and optical characterization of silicon material including: low temperature Fourier Transform Infrared (FTIR) absorption spectroscopy; variable temperature Hall-effect analysis; photo-Hall; photoluminescence; and photothermal ionization. A short description and a discussion of the effectiveness and limitations of each of these techniques can be found in NMAB Report #362 by the National Materials Advisory Board (Reference 1). Each technique has some special advantage over the other for obtaining specific types of information. For instance, Hall analysis can be used to directly measure the concentration and activation energies of the impurities, while FTIR spectroscopy can only be used to directly measure the impurities' presence, but not concentration. Also, FTIR measures only optically active impurities while Hall-effect measures only electrically active impurities. This report examines the electrical transport Hall and the optical FTIR analysis techniques and

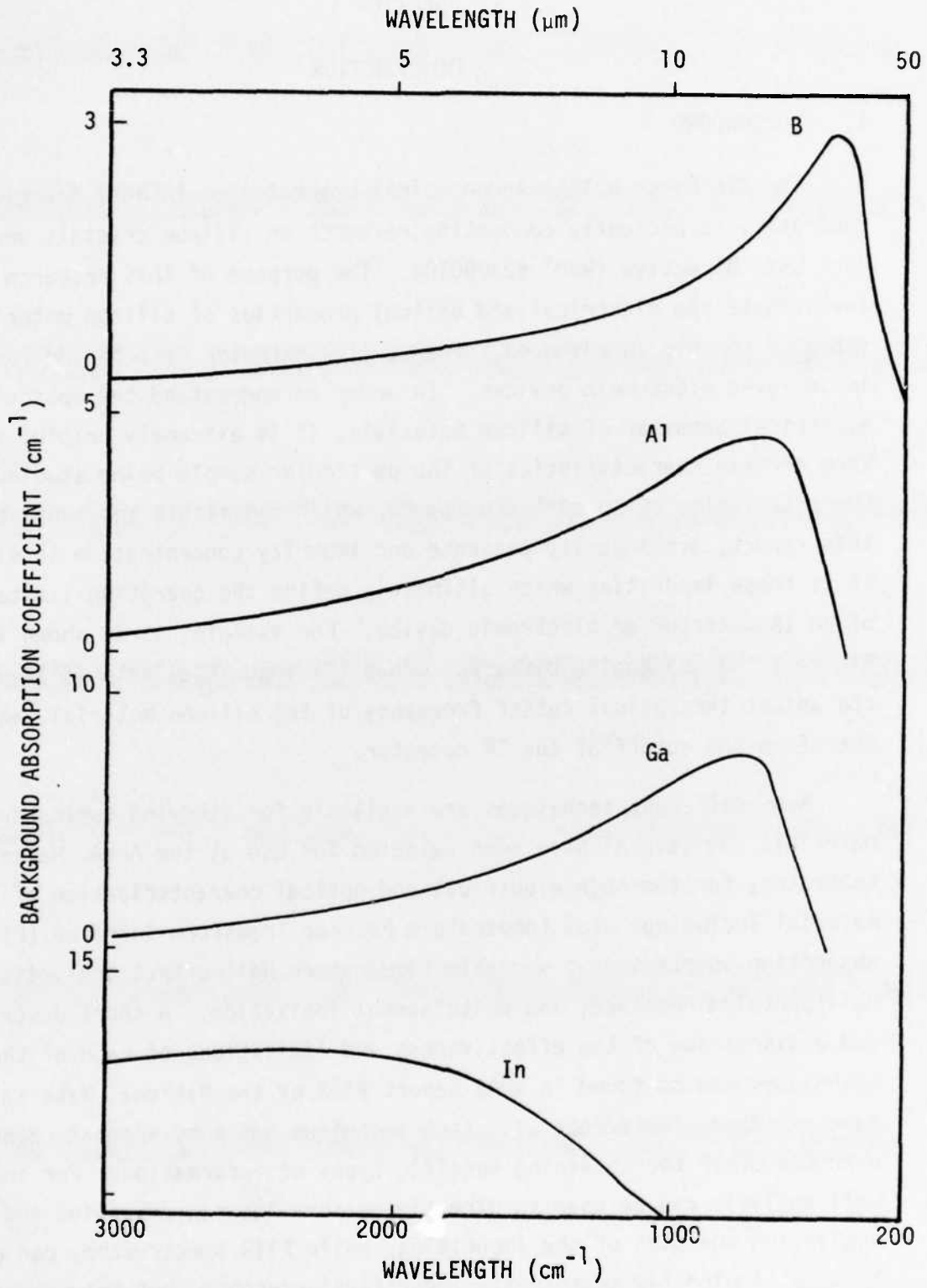


Figure 1. Photoionization Absorption of Group III - Doped Silicon

accurately determines the coefficients that couple the two methods. These results permit using the advantages of each method in routine sample analysis, namely, the speed and convenience of FTIR and the quantitative output of the Hall measurements.

Absorption spectroscopy is one of the oldest and most understood techniques and therefore one of the more widely accepted techniques for studying impurities in silicon. Fourier transform spectroscopy is a modern improvement of the older technique which incorporated the use of prisms and gratings. The birth of the minicomputer and the Fast Fourier Transform made possible the more widespread use of FTIR spectroscopy, which has advantages in speed and resolution over the older absorption experiments. In either the older or more modern version, absorption spectroscopy measures the strength of atomic and molecular transitions produced by an interaction between the sample material and the light illuminating the sample. Each atom or molecule produces a unique spectral pattern (or fingerprint) which enables spectroscopists to distinctly identify a particular atom or molecule in the sample being tested.

Probably the most studied impurities in silicon are the Group III and Group V elements along with carbon and oxygen. The Group III and Group V impurities give rise to electronic transition spectra while carbon and oxygen give rise to local-mode vibrational spectra.

The absorption spectra of all of the previously mentioned elements in silicon can be observed using FTIR spectroscopy. While the main emphasis of this report is on the Group III elements boron, gallium, and indium, the other elements cannot be ignored because of their interference in measurements of the Group III elements. This technique has been successful in measuring Group III elemental impurities in silicon even at low concentrations of the part per billion (PPB) level. To make this experiment quantitative, it must be calibrated against another technique such as Hall-effect analysis or neutron activation analysis (NAA). Further description of the calibration procedure can be found in Section II.

## 2. PROBLEM

Thus, the problem of this report is to experimentally determine optical calibration constants for boron, gallium, and indium elemental impurities in silicon. These calibration constants will be used with FTIR absorption spectroscopy to accurately measure the concentration of these impurities.

Since it is essential to know under what experimental conditions the constants may be used, an integral part of the problem is to define the following:

- The temperature range over which the new calibration constants may be used
- The concentration range over which the constants are valid
- The usefulness of these calibration constants in multiply-doped silicon samples

Two additional problems that will be included in this report are the assignment of new line positions, line spacings, etc. to the Group III acceptors, and the calibration of the oxygen lines at  $1136 \text{ cm}^{-1}$  and  $1128 \text{ cm}^{-1}$  as a means to ensure that the sample temperature as measured by the temperature sensor is correct (Reference 2).

## 3. APPROACH

The first and most important step in this study was to put together a set of Group III-doped silicon samples. To perform a study like this, it was necessary to have access to either a crystal growing facility or a facility with an inventory of a wide variety of Group III - doped silicon crystals. At least three doped silicon crystals were needed for each Group III element to be studied. These three crystals must represent a range of dopant concentrations. The Materials Laboratory had available the samples which were used in this study. Some of these crystals had previously been measured for impurity concentrations. Others had only resistivity measurements provided by the manufacturer which could be related to impurity concentration by Sclar's concentration versus resistivity curves (Reference 3). A knowledge of approximate dopant concentration was required for sample selection. These samples were

then cut to appropriate dimensions and polished for each experimental technique included in this study. Measurements were then taken on these samples by FTIR absorption spectroscopy, variable temperature Hall-effect analysis, and neutron activation analysis. Hall-effect analysis and neutron activation analysis provided two independent measurements of impurity concentrations for each sample.

FTIR absorption spectroscopy measurements provided information such as peak areas, peak locations, line spacings, etc. on each Group III-doped silicon sample. Data was taken at a variety of sample temperatures to determine the effect of temperature variation on peak shape. At least one sample was run over a temperature range of 5 - 77<sup>0</sup>K to provide the temperature dependence of the oxygen lines at 1136 cm<sup>-1</sup> and 1128 cm<sup>-1</sup>. Knowing the temperature dependence of these lines will provide a means to roughly measure actual sample temperature.

A multiply-doped silicon sample was analyzed by each technique to test the ability to use calibration constants for samples with more than one Group III impurity present.

#### 4. SCOPE

Although calibration constants are needed for the Group III, Group V, oxygen, and carbon impurities in silicon, this report was limited to the study of only the Group III elemental impurities, boron, gallium, and indium in silicon. Very few thallium-doped silicon samples exist and therefore were not included. An aluminum-doped silicon sample was measured optically but neither Hall nor NAA measurements could be obtained.

Calibration constants were obtained for sample temperatures between 5<sup>0</sup>K and 12<sup>0</sup>K. These are the most common temperatures attainable by the cooling systems at the Materials Laboratory.

Because of the limited sample selections, in some cases only a narrow range of dopant concentration could be found.

This report is intended to be experimental in nature. A great deal of theory already exists which explains acceptor defects in silicon and will be referred to when necessary for discussion.



The main emphasis of this report was on the FTIR absorption spectroscopy portion of this study. Little discussion will appear on Hall analysis and Neutron activation analysis. Theoretical discussion focuses on the optical properties of these materials as they affect the absorption measurements.

## 5. ASSUMPTIONS

It should be noted that two major assumptions were made throughout this work. These assumptions were:

- a. In this study, each piece of material was sliced into no more than three samples. These three samples were then distributed, one for FTIR absorption spectroscopy, the second to Hall analysis, and the third to neutron activation analysis. Ideally, all three measurements should be made on one sample. This would eliminate the possibility of there being any concentration gradients from one sample to the next. For cases when one sample could not be used for each measurement, it was assumed that an adjacent sample from the same piece of material had the same impurity concentration.
- b. Reflectance measurements were not made on samples as part of this study. A simple visual inspection was made to ensure all samples had a highly polished surface. The reflectivity was assumed to be .28 for all samples.

## SECTION II

IR ABSORPTION SPECTRA OF GROUP III  
ACCEPTORS IN SILICON AND THEIR USE IN QUANTITATIVE MEASUREMENTS

## 1. INTRODUCTION

The Group III acceptor lines have been used in the past to measure impurity concentrations in silicon crystals (References 4, 5, 6). A great deal of experimental and theoretical work has been done to explain the physical origin of these lines. This section will provide the reader with a brief description of these excitation lines as developed by theory along with recent experimental results. With this basic understanding of the acceptor lines, an explanation of how these lines can be calibrated to yield impurity concentration measurements will be presented. The calibration constants reported by various investigators are not in close agreement (References 5, 7). Factors which could influence the shapes of these spectral lines must be considered when making quantitative measurements. These factors include phonon broadening, electric field broadening, concentration broadening, and stress and strain broadening. The conditions under which these broadening mechanisms occur will be pointed out as situations to avoid when making quantitative measurements and as a possible explanation for previous discrepancies in reported calibration constants. Finally, the reasons why the existing calibration factors of Honeywell (Reference 4) were difficult to use, will be discussed.

## 2. GROUP III ACCEPTOR IR SPECTRA

Group III elements normally occupy substitutional sites in the silicon lattice. Having only three valence electrons, they are not able to participate in all four valence bonds available at each substitutional site. This electron deficiency at the acceptor site is referred to as a hole. Holes act as positively charged particles and are loosely bound to the negatively charged acceptor ion core. At room temperature, holes are ionized from their acceptor sites and are free to move in the crystal as charge carriers. At low temperatures, around  $10^0\text{K}$ , holes tend to occupy the lowest bound energy state. Interaction of these holes with IR radiation causes effective mass type excitation spectra (References 8, 9, 10, 11).

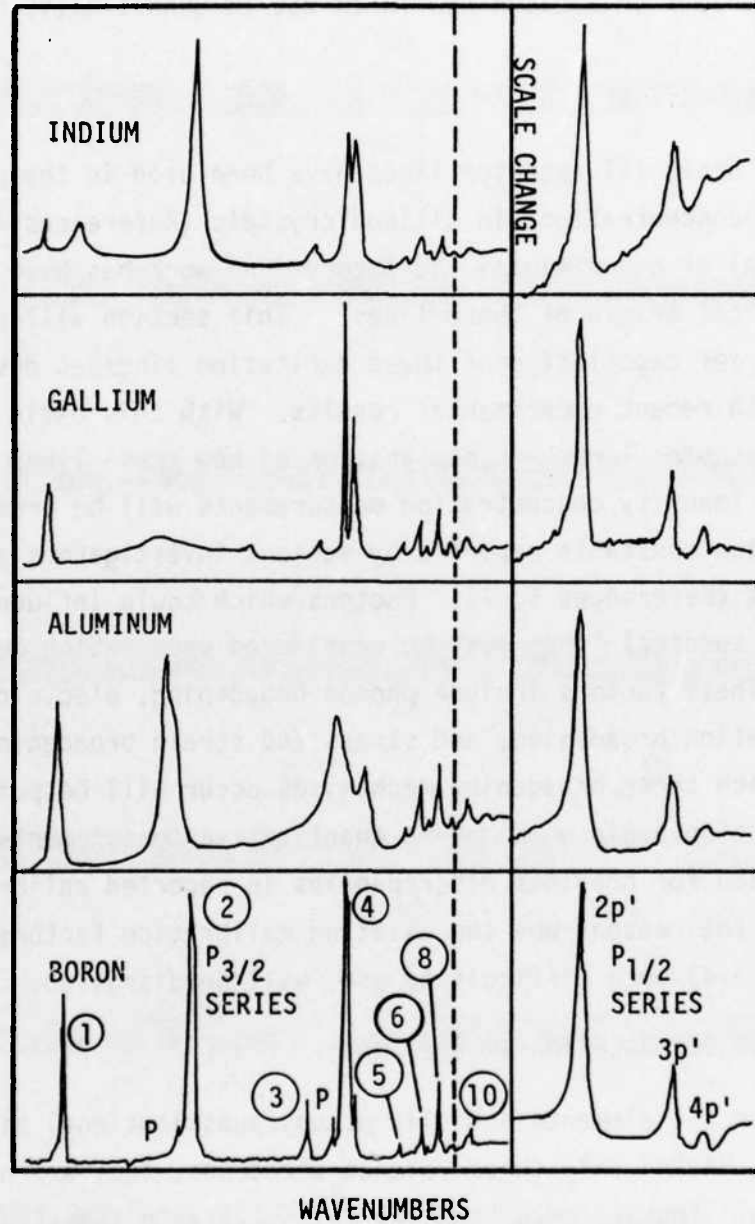


Figure 2. Comparison of Acceptor Spectra In, Ga, Al, and B

The spectra arise due to transitions from an s-like ground state to p-like excited states. Because only the s-like ground state wave function penetrates the acceptor ion core, only the ground states are affected by the atomic differences of the various acceptors. P-like excited states, as calculated by effective-mass theory, are identical for all acceptors. This similarity in the p-states for all the acceptors results in a characteristic pattern for all acceptor spectra. The various acceptor ground states are shifted in energy due to the differences in local screening of the s-state. The similar spectral pattern of the Group III acceptors In, Ga, Al, and B can be seen in Figure 2 which shows spectra obtained in this study. Here the  $p_{3/2}$  series are lined up on line 9 and the  $p_{1/2}$  series are lined up on line 2p'. Enlargements of these spectra will be provided in Section IV to show more detail and to provide exact energy locations. These hole transitions can be seen with reference to the silicon valence bands in Figure 3. In the case of the  $p_{3/2}$  series, the top of the valence band is the series limit. The top of the spin orbit split-off valence band is the  $p_{1/2}$  series limit.

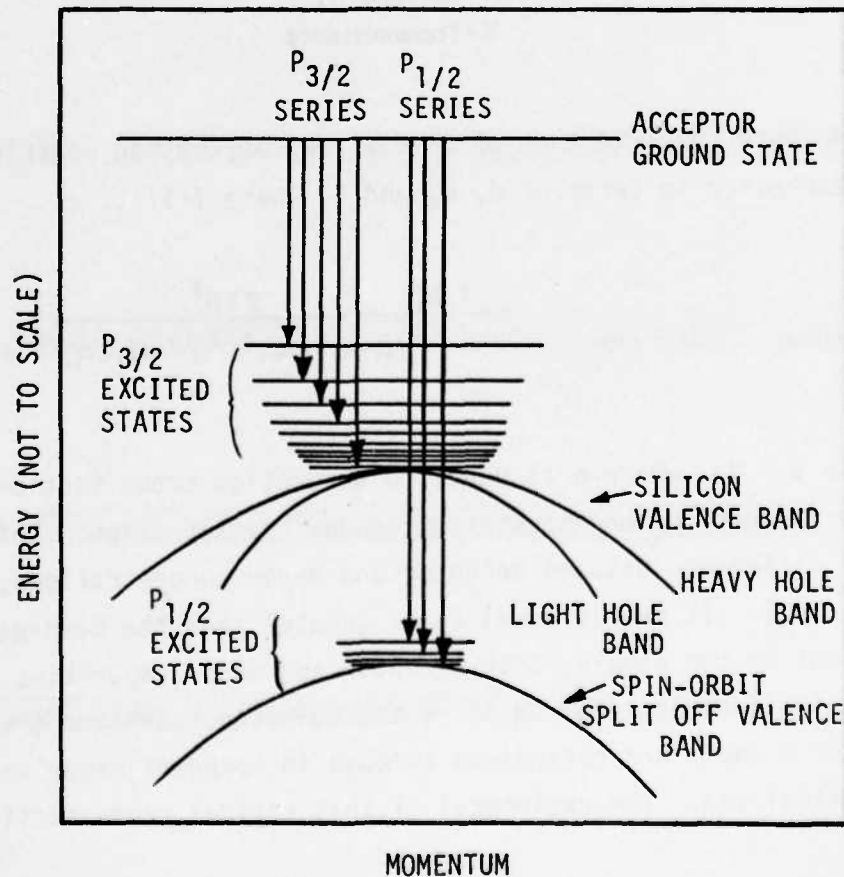


Figure 3. Band Diagram of Acceptor Transitions in Silicon

## 3. USING SPECTRAL LINES TO MAKE QUANTITATIVE MEASUREMENTS

The ability to make quantitative measurements using absorption spectroscopy relies on the Beer's Law dependence of line intensity to concentration.

Beer's Law

$$I = I_0 e^{-ad}$$

where

$I_0$  = Intensity of radiation incident on sample

$I$  = Intensity of radiation after passing through sample

$a$  = Absorption coefficient

$d$  = sample thickness

Taking into account multiple internal reflections within the sample, Beer's law becomes (Reference 12),

$$I = I_0 \frac{(1-R)^2 e^{-ad}}{1 - R^2 e^{-2ad}}$$

$R$  = Reflectivity

$T$  = Transmittance

Using the more complete form of Beer's law, absorption coefficient can now be expressed in terms of  $d$ ,  $R$ , and  $T$ , where  $T = I/I_0$ , as

$$a = \frac{1}{d} \ln \left[ \frac{2TR^2}{[(1-R)^4 + 4T^2R^2]^{1/2} - (1-R)^2} \right]$$

Also  $a = N\sigma$ , where  $\sigma$  is equal to absorption cross section and  $N$  is equal to the net, or uncompensated, dopant concentration. This observed  $N$  is the difference between acceptor and donor concentrations,  $N = [N_a - N_d]$ . If energy equal to or greater than the band gap energy is incident on the sample, both acceptor and donor impurities can be seen. This is often referred to as the Kolbesen technique (Reference 6). After  $N$  and  $a$  are determined through independent experiments,  $\sigma$  can be calculated. The reciprocal of this optical cross section is then

used as the calibrated constant which relates the absorption coefficient to concentration.

$$1/\sigma = k \text{ so that } ak = N$$

A feature from an acceptor absorption peak must be then selected as the value for  $a$ . In the past  $a$  has been equated to peak height or peak area (References 4, 5). It is common to use peak area for peaks with a measurable half-width, whereas for narrow spectral lines it is common to use peak height. Most Group III acceptor lines have an adequate half-width and therefore peak areas are normally used to characterize acceptor lines.

The line widths and peak shapes of the acceptor lines being studied are subject to distortion by various mechanisms. Such peak distortions can then lead to inaccuracy in concentration measurements. When making quantitative measurements, awareness of these sources of peak distortion is necessary for proper interpretation of spectral information. The mechanisms which affect the shape of acceptor lines include phonon or thermal broadening (References 13, 14, 15); concentration broadening (which is due to overlap of the wave functions of bound carriers) (Reference 16); internal electric field broadening (References 17, 18); internal and external stress and strain broadening (References 4, 19); and instrumental broadening (Reference 19).

Because of thermal broadening, absorption measurements should only be taken on samples cooled to below 40°K. Above this temperature, acceptor lines begin to broaden considerably which can lead to inaccuracy in quantitative optical measurements. Resonant interaction of phonons with acceptor energy transitions causes a drastic distortion or even complete disappearance of acceptor spectral lines. This effect is seen in line 2 of gallium and line 3 of aluminum. In this study, phonon-coupled lines will be avoided for use due to the anomalous behavior these lines exhibit.

Concentration effects on peak half-widths are known to occur at concentrations as low as  $1 \times 10^{15} \text{ cm}^{-3}$ . At concentrations above  $10^{18} \text{ cm}^{-3}$ , line structure is completely destroyed (References 13, 16). J.J. White shows that half-widths vary with the cube root of concentration.

How this variation affects peak area will affect the linear relationship of the calibration constant with concentration. For this study, an initial assumption will be made that peak area is linearly proportional to concentration. The validity of this assumption will be evaluated while interpreting the experimental results.

Internal electric field effects on boron acceptor spectra were studied by J.J. White in 1967. He observed the effects of coulombic fields caused by ionized impurities (References 13, 18). The effects due to ionized impurities are negligible at temperatures below 40<sup>0</sup>K in comparison to phonon broadening. Since all samples in this study were measured at temperatures well below 40<sup>0</sup>K, this effect was ignored.

Strain broadening can be caused by crystalline imperfections such as the presence of impurities or dislocations. Modern crystal growth techniques reduce dislocation concentration to levels where dislocation broadening is small. Special care must be taken to eliminate any accidental stress broadening caused by sample mounting.

Instrumental broadening is negligible if the observed full-width at half maximum,  $W_{1/2}$ , is at least twice as large as the instrumental half-width. This criterion is met when studying acceptor lines using a resolution of 0.5  $\text{cm}^{-1}$  (References 19, 20).

#### 4. PROBLEMS WITH PREVIOUS CALIBRATION FACTORS

Workers from Honeywell Corporate Research Center (Reference 4) have done a calibration study resulting in the most recent calibration constants which relate peak height and/or peak area obtained by absorption spectroscopy to concentrations obtained using room-temperature Hall coefficient and resistivity measurements. Calibration constants developed by Honeywell under DARPA contract #DAAK70-77-C-0194 are listed in Table 1.

These calibration constants have often been used at the AFWAL Materials Laboratory, but in many cases their use became difficult. Because of these difficulties, this report was undertaken to develop new calibration constants. The particular cases where the already existing calibration constants could not be used or their use was questionable are listed in the following paragraphs.



TABLE 1

## OPTICAL CALIBRATION CONSTANTS AT 8K (Reference 4)

Impurity	Line (cm <sup>-1</sup> )	Concentration (cm <sup>-3</sup> )
Boron	279	[B] = peak area/6.6 X 10 <sup>-14</sup>
Boron	666	= area/6 X 10 <sup>-15</sup>
Aluminum	472	= area/2.4 X 10 <sup>-14</sup>
Gallium	510	= area/2 X 10 <sup>-14</sup>
Indium	1175	= area/5 X 10 <sup>-16</sup>
Thallium	1907	= area/8.5 X 10 <sup>-17</sup>
Carbon	600	= peak X 6.7 X 10 <sup>16</sup>
Oxygen	1136	= peak X 3.09 X 10 <sup>16</sup>
B-X	184	= area/9.5 X 10 <sup>-14</sup>
Al-X	373	= area/4 X 10 <sup>-14</sup>
Ga-X	381	= area/4 X 10 <sup>-14</sup>
In-X	830	= area/3.5 X 10 <sup>-15</sup>
Phosphorus	315	= area/9.94 X 10 <sup>-14</sup>

a. Anytime the transmittance of the spectral line being used for calibration goes to zero, due to either high concentration or excessive sample thickness, calibration constants are no longer reliable. See Figure 4 for examples. For gallium and aluminum, the primary line used for calibration by Honeywell was line 2 of the  $p_{3/2}$  series. This is the most intense spectral line of In, B, and Al, and is therefore the most practical to use in calibration, except in the cases presented. A secondary line must therefore be used for calibration purposes.

b. The extremely distorted shape of line 2 of the gallium  $p_{3/2}$  spectra and the absence of line 3 in the aluminum  $p_{3/2}$  spectra are due to a strong coupling to the 519 cm<sup>-1</sup> phonon as suggested first by Onton et al (Reference 21), and later shown theoretically by Chandrasekhar (Reference 22). The distortion of these lines is shown in Figure 4. The existing Honeywell calibration constant for gallium in silicon references this distorted line 2 of gallium. Since line 2 of gallium is strongly coupled to this phonon, and therefore to the silicon lattice, it is sensitive to stress induced on the material. Stress can be induced

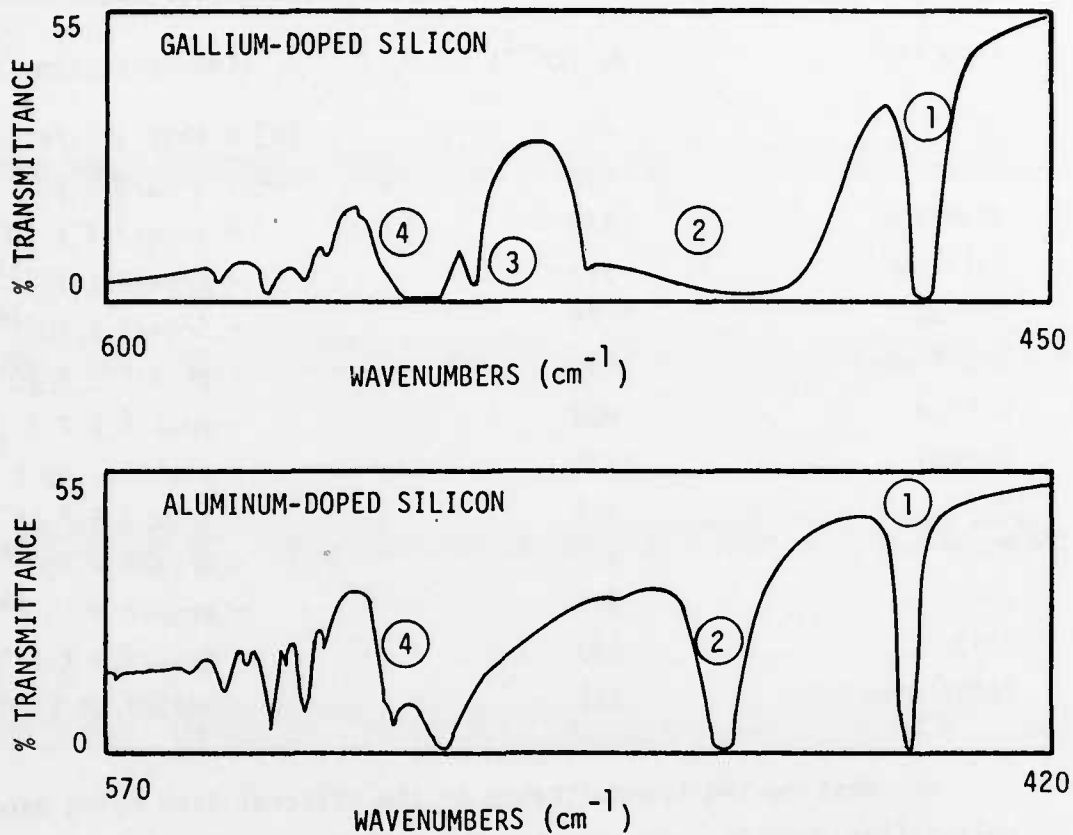


Figure 4. Transmittance Spectra of Gallium and Aluminum Doped into Silicon (Line 2 of these spectra has become saturated due to either excessive sample thickness or high dopant concentration. Ga line 2 is distorted and Al line 3 is missing due to coupling with the 519 cm<sup>-1</sup> phonon.)

purposely through mechanical means or accidentally by careless sample mounting. Extreme care must be taken while mounting samples to avoid the differential contraction of the copper sample holder and the silicon sample during cooling. Other processes which also occur near line 2 are oxygen and boron local mode absorptions. Because of the rather complex nature of line 2 of the gallium spectrum, another line of the  $p_{3/2}$  spectrum or a line of the  $p_{1/2}$  spectrum should be used instead as a reference line for measuring gallium concentration.

c. Another case encountered is the inability to obtain precise temperature control. Honeywell's calibration constants were determined

for a sample temperature of 8<sup>0</sup>K. Some cooling systems are capable of attaining temperatures no lower than 12<sup>0</sup>K. Others cool the sample to below 6<sup>0</sup>K. For now, 8<sup>0</sup>K calibration constants must be used for sample temperatures ranging from 5<sup>0</sup>K to 15<sup>0</sup>K. Obviously research is necessary to define the usable range of each calibration constant. Shown in Figure 5 is the temperature variation of the  $p_{1/2}$  lines of boron between 6<sup>0</sup>K and 15<sup>0</sup>K which clearly demonstrates the need for accurate temperature control.

Most of these difficulties with the existing calibration constants can be remedied by selecting a different spectral line for use in measuring impurity concentration. This requires a concentration dependence study involving FTIR absorption spectroscopy and another technique such as Hall analysis or Neutron activation analysis.

Although Hall-effect analysis is the more accepted means for determining impurity concentrations, FTIR absorption spectra along with existing calibration constants are often used to obtain impurity concentrations for comparison. Sometimes, concentrations obtained by absorption spectroscopy correspond quite well with concentrations determined by Hall analysis. This has been especially true in the case of Honeywell's indium calibration constant (Reference 4). Conflicting results between these techniques, however, produce concern as to whether the measurements were made correctly or if the calibration constants being used are inaccurate.

To summarize, a need for a study to produce new calibration constants for the Group III acceptors in silicon exists at the Materials Laboratory. This need has come about through unsatisfactory use of existing calibration constants and through conflicting comparisons between Hall and FTIR absorption. An understanding of why these two techniques at times produce conflicting information is essential to further understand the electrical and optical properties of silicon materials being studied. Thorough knowledge of impurity presence and impurity concentration is necessary for understanding the electrooptical properties of these materials.

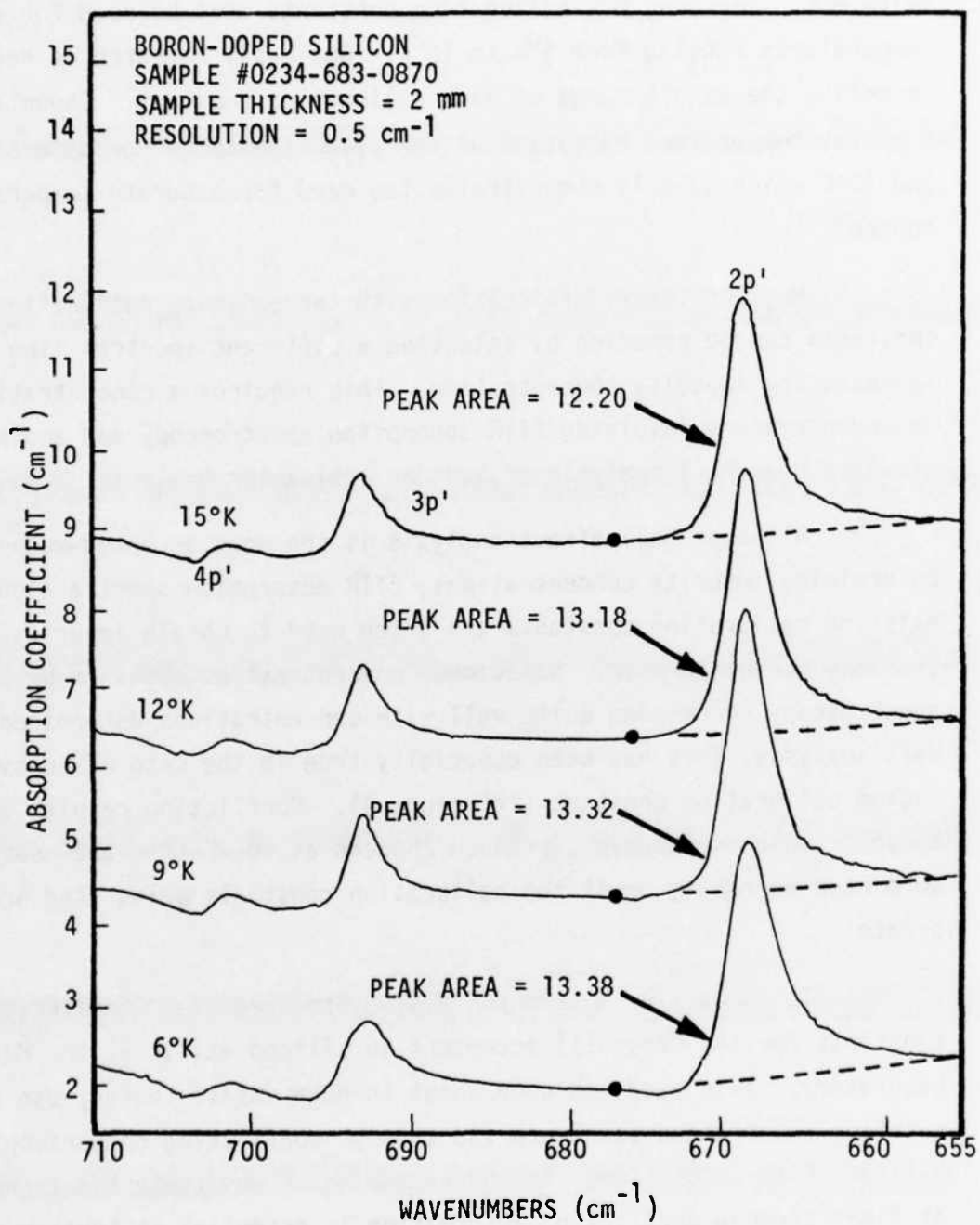


Figure 5. Temperature Dependence of the Boron p<sub>1/2</sub> Lines  
 (Areas are determined using a computer integrating routine available with the Digilab system.)

## SECTION III

## EXPERIMENTAL EQUIPMENT, MATERIALS, AND PROCEDURES

## 1. INTRODUCTION

Since this report focuses on the FTIR absorption spectroscopy portion of this study, only the FTIR absorption experiment will be discussed in detail. However, at the end of this section, comments will be made on the Hall-effect and neutron activation measurements.

## 2. EXPERIMENTAL EQUIPMENT

Spectroscopic measurements have been made using a Digilab Model FTS-20CVX Fourier Transform spectrometer. The spectrometer includes a Model 146 Bloch interferometer with a globar source and a cesium iodide (CsI) beamsplitter. Also a CsI windowed Triglycerin Sulfide (TGS) detector was used to allow investigation in the spectral region from  $3600 \text{ cm}^{-1}$  to  $220 \text{ cm}^{-1}$ . Wavenumber locations were identified by the spectrometer using a reference interferometer which included a HeNe laser and white light source.

The sample compartment of the spectrometer was modified to accommodate the several cryogenic cooling systems used in this study (Figure 6). A special isolation table was designed to hold the closed cycle cooling system, Cryodyne Cryocooler, in the sample compartment. This isolation table, shown in Figure 6, prevents any vibrations created by the closed cycle system from transferring to the optical bench of the spectrometer.

The data system by Digilab included a Nova 3 minicomputer, a Hewlett Packard CRT display scope, a Silent 700 keyboard/printer, and a Houston plotter. The spectra produced were digitized and stored on magnetic disk cartridges using a Data General dual disk drive unit.

Several cryogenic sample-cooling systems were used in this study. They included:

- a. A Sulfrian Cryogenics 2-liter liquid helium optical-dewar. This was used for constant temperatures of 5 or  $12^{\circ}\text{K}$ .

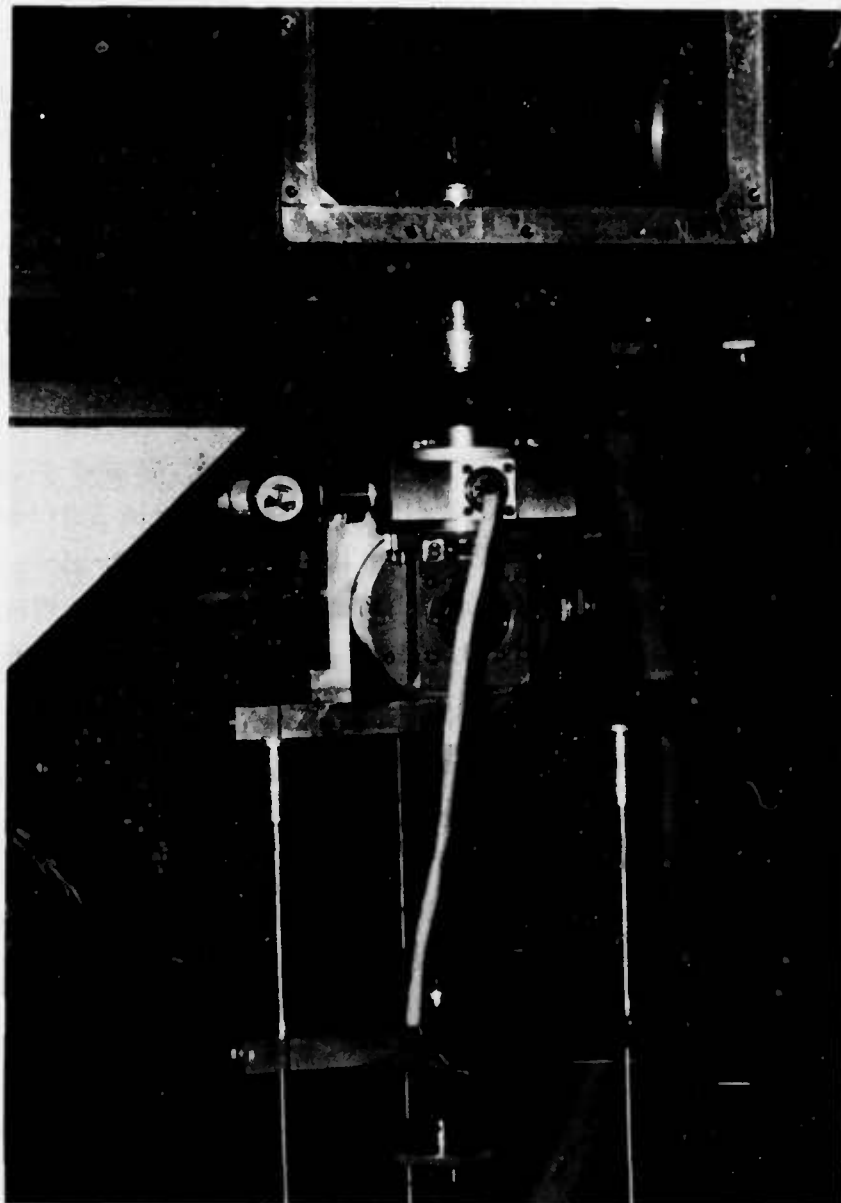


Figure 6. Modified Sample Compartment and Isolation Table

- b. An Air Products and Temperature Inc. Model LT-3-110 liquid helium transfer Heli-Tran refrigerator. Temperatures were manually controlled by the Model OC-20 Cryo-Tip control panel. This controlled temperatures between 5 and 300<sup>0</sup>K with an accuracy between  $\pm 0.02$  to  $\pm 1.0^0$ K.
- c. A Model 21SC Cryodyne Cryocooler closed-cycle refrigeration system. The cold head portion was equipped with a vacuum shroud designed and built at the Materials Laboratory. The Lake Shore Cryotronics Model DRC-7C Digital Cryogenic Thermometer/Controller was used with the cryocooler, and incorporated the use of a silicon diode for sensing temperature. This system could be used between 9 and 300<sup>0</sup>K. The controllability of this system was  $\pm 0.5^0$ K. This system added 60 cycle noise to spectra around 400  $\text{cm}^{-1}$ .

All three of these cryogenic cooling systems were equipped with oxygen free high conductivity (OFHC) copper sample holders. To each copper sample block was attached a silicon-diode temperature sensor. For the cryocooler system, a Lake Shore Model DT-500 CU-DRC-B sensor was used and for the other two systems Model DT-500 P sensors were used. A current supply and digital voltmeter were required for use with the silicon diode sensors. CsI windows were mounted using a black wax to the vacuum shrouds of all three cooling devices to allow transmittance through the vacuum shrouds.

### 3. MATERIALS

The doped silicon samples used in this study were grown by various techniques including standard Czochralski (CZ), float zoning (FZ), and cold crucible or skull. The materials were supplied to the Materials Laboratory by Honeywell, Hughes, Spectrolab, Aerojet, Monsanto, Westinghouse, Dow Corning, Ceres, and Shin Etsu Hondotai (S.E.H. from Japan). These samples represent most of the common crystal growth/doping methods used today. This variety of samples will test the reliability of the use of calibration constants for all the different types of doped silicon materials listed above.



All the samples were cut and polished at the Materials Laboratory. After the samples were cut and polished, they were issued an identification number for future reference. The samples used in this study are listed in Table 2 which shows the sample identification number, the Group III majority impurity, the manufacturer, the growth technique and the approximate impurity concentration.

#### 4. FTIR ABSORPTION SPECTROSCOPY

The doped single-crystal samples were cut, tapered, polished, and then mounted to the OFHC copper cold tip of the various cryogenic systems (Figure 7). Using a thin layer of vacuum grease which contained silver powder, the samples were thermally contacted to the copper tips. Special care was taken not to stress the sample while mounting. The grease was applied to only one corner of the sample to minimize the differential contraction between the cold tip and the sample while cooling. Samples less than 2 mm thick were especially vulnerable to this type of stress. The spectra produced from the sample was immediately checked for any evidence of stress such as abnormal line broadening or splitting. If the spectra exhibited any stress characteristics, the sample was remounted until it produced sharp, unbroadened excited state lines. Several other workers have encountered sample stress due to careless mounting and have described different techniques used to minimize this problem (References 13, 16, 19).

After samples were carefully mounted, they were cooled to between 5 and 8<sup>0</sup>K. The sample temperatures were monitored using silicon diode sensors which were attached to the copper cold tips. Temperatures were verified approximately by comparing relative peak heights of the oxygen 1136 cm<sup>-1</sup> and 1128 cm<sup>-1</sup> lines (Reference 2). Figure 8 shows a curve of the relative oxygen peak intensities as a function of temperature. Use of this curve provides an excellent way to determine if sufficient thermal contact has been made between the sample and cold tip.

All spectra were taken at a resolution of 0.5 cm<sup>-1</sup> and recorded using a Digilab Model FTS-20CVX Fourier Transform spectrometer purged with dry nitrogen. This spectrometer was calibrated using known in vacuo

TABLE 2  
 INFORMATION ON SAMPLES USED IN THIS STUDY

SAMPLE ID #	MANUFACTURER	GROWTH METHOD	PRIMARY DOPANT	APPROX. CONC. ( $\text{cm}^{-3}$ )
0119-757-0923	Monsanto	Float Zoned	Boron	$5 \times 10^{14}$
0118-755-0917	Monsanto	Float Zoned	Boron	$4 \times 10^{14}$
657	RADC*-Ceres	Cold Crucible	Boron	$1 \times 10^{15}$
0234-683-0870	Shin Etsu Hondotai	Float Zoned	Boron	$3 \times 10^{15}$
026-101-0861	Texas Instru.	Float Zoned	Aluminum	$5.5 \times 10^{15}$
044-142-0619	Hughes	Float Zoned	Gallium	$1 \times 10^{16}$
0102-295-0621	Hughes	Float Zoned	Gallium	$4 \times 10^{16}$
987	Spectralab	Float Zoned	Gallium	$1 \times 10^{15}$
0109-285-0956	Aerojet	Czochralski	Indium	$1 \times 10^{17}$
0103-297-0233	Westinghouse	Float Zoned	Indium	$2.4 \times 10^{16}$
011-796-0952	Dow Corning	Float Zoned	Indium	$5 \times 10^{16}$

\*Rome Air Development Center

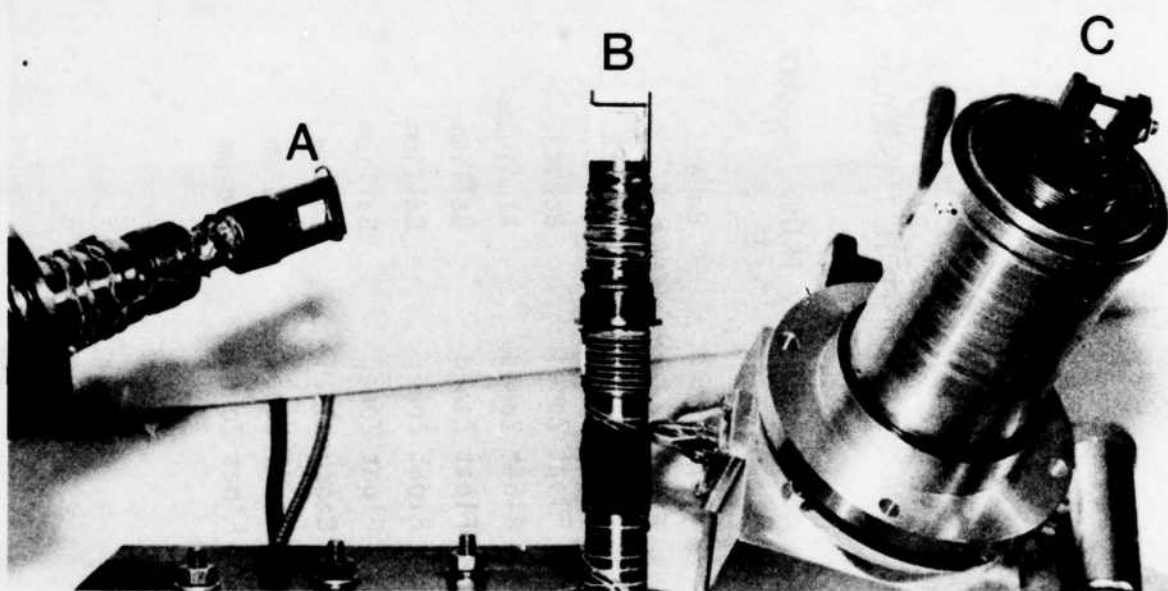


Figure 7. Sample Holders Used for Different Cooling Systems

A	Liquid-helium optical dewar	7/16 by 5/16 inches
B	Heli-tran cold tip	3/8 by 3/8 inches
C	Closed cycle system	7/16 by 7/16 inches

positions of water vapor and carbon dioxide absorption bands (Reference 23). Lines measured deviated from the standard values by  $-0.03 \text{ cm}^{-1}$  to  $0.00 \text{ cm}^{-1}$  throughout the regions where data was reported.

Transmittance values were then obtained using the air reference, stored-ratio, single beam method. The sample transmittance was referenced to an empty cryocooler. This method can be extremely inaccurate photometrically, if care is not taken to place the empty sample holder in exactly the same location it was while the sample was being analyzed. The difficulty of this task is increased when using bulky cryogenic sample cooling systems. It is advisable to check transmittance values obtained to values shown in the literature, especially if the literature transmittance spectra were obtained with a double beam instrument which could be photometrically calibrated prior to each experiment. Transmittance values were transformed to absorption coefficient values using the equation,

$$a = \frac{1}{d} \ln \left[ \frac{2TR^2}{[(1-R)^4 + 4T^2R^2]^{1/2} - (1-R)^2} \right]$$

a = Absorption Coefficient

d = sample thickness

R = Reflectivity

T = Transmittance

Peak areas are measured using an integrating program included with the Digilab software package. This routine integrates the area between the peak and a baseline which is designated by the user.

## 5. HALL-EFFECT ANALYSIS

Hall measurements were made at the AFWAL Materials Laboratory by personnel experienced in the technique. These measurements were done with a variable-temperature Hall-effect system. Samples were cut into the van der Pauw configuration (Reference 24). Data was then analyzed in the normal manner by fitting the charge balance equation and using the Lang mass and an empirical r-factor (References 25, 26, 27).

6. NEUTRON ACTIVATION ANALYSIS

Indium and gallium doped silicon samples were sent to the University of Missouri Research Reactor for analysis. Boron and aluminum doped samples could not be measured using the technique. Concentrations of indium and gallium impurities in these samples were reported with an accuracy of +5%.

## SECTION IV

## EXPERIMENTAL RESULTS AND DISCUSSION

## 1. INTRODUCTION

Presented here are the experimental results from FTIR absorption spectroscopy, Hall analysis, and neutron activation analysis (NAA). Results from these three measurements are combined to obtain the new calibration relationships. Here a detailed description of the new relationships will be given along with any limitations for their use. A discussion on the results of high resolution absorption measurements will be given but will be limited so as not to detract from the main theme which is on calibration relationships. A more complete description of these results can be found in the appendix.

## 2. ABSORPTION SPECTRA

High resolution FTIR absorption spectroscopy measurements were made on indium, gallium, aluminum, and boron in silicon. All  $p_{3/2}$  and  $p_{1/2}$  excited state energies were carefully measured. Sharp line  $p_{3/2}$  and  $p_{1/2}$  excited state spectra are shown in Figures 8 through 11. All reported acceptor lines are shown along with some previously unreported acceptor related lines. These new acceptor related excited energy states were seen in the  $p_{3/2}$  spectra of indium, gallium, aluminum, and boron. A  $5p'$  line was observed for the first time in the gallium  $p_{1/2}$  spectra. A renumbering of the boron lines was required so that the boron spectra would correspond to the accepted numbering convention of the other Group III acceptor spectra. A feature in each acceptor  $p_{3/2}$  spectrum was defined as the ground state binding energy  $E_I$ , and the spin-orbit splitting of the valence bands was measured.

Discussion of these results can be found in the appendix of this report which contains a paper that has been submitted to Physical Review. These results come directly from this work and are important results, but because they do not add to the discussion on calibration relationships, they were not included in the main text.

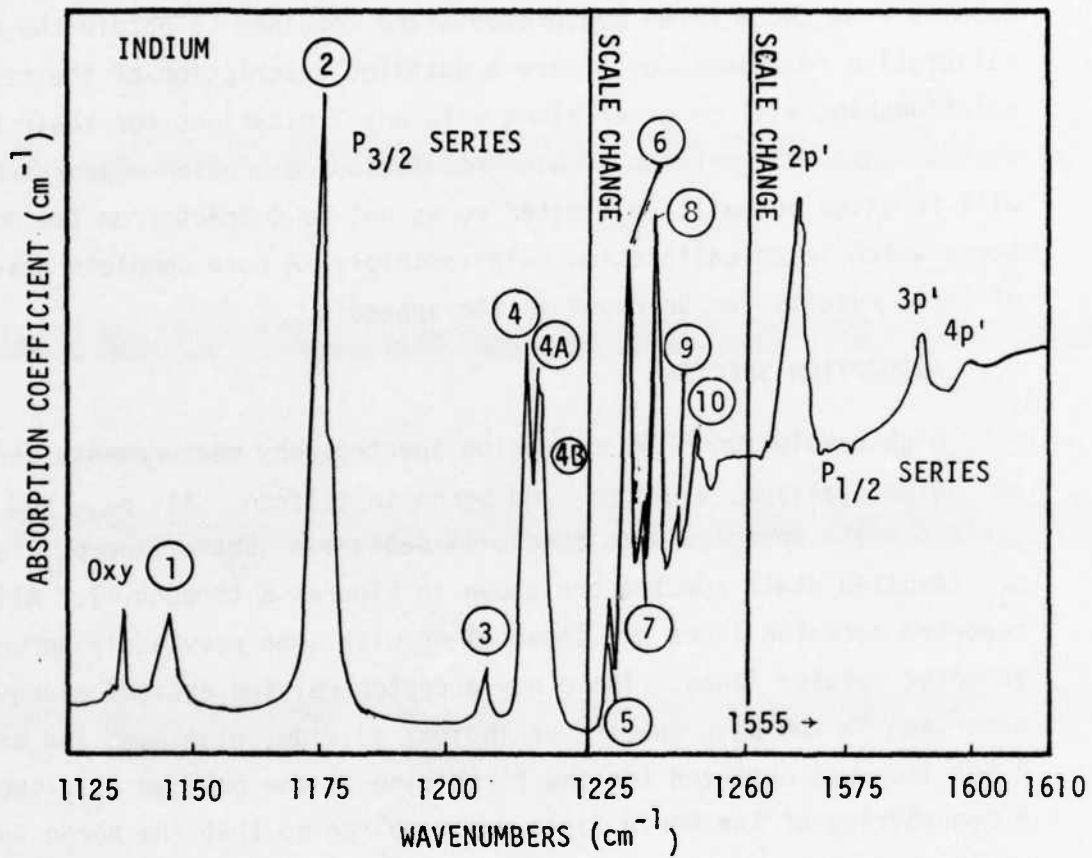


Figure 8. IR Absorption Spectrum of Indium-Doped Silicon



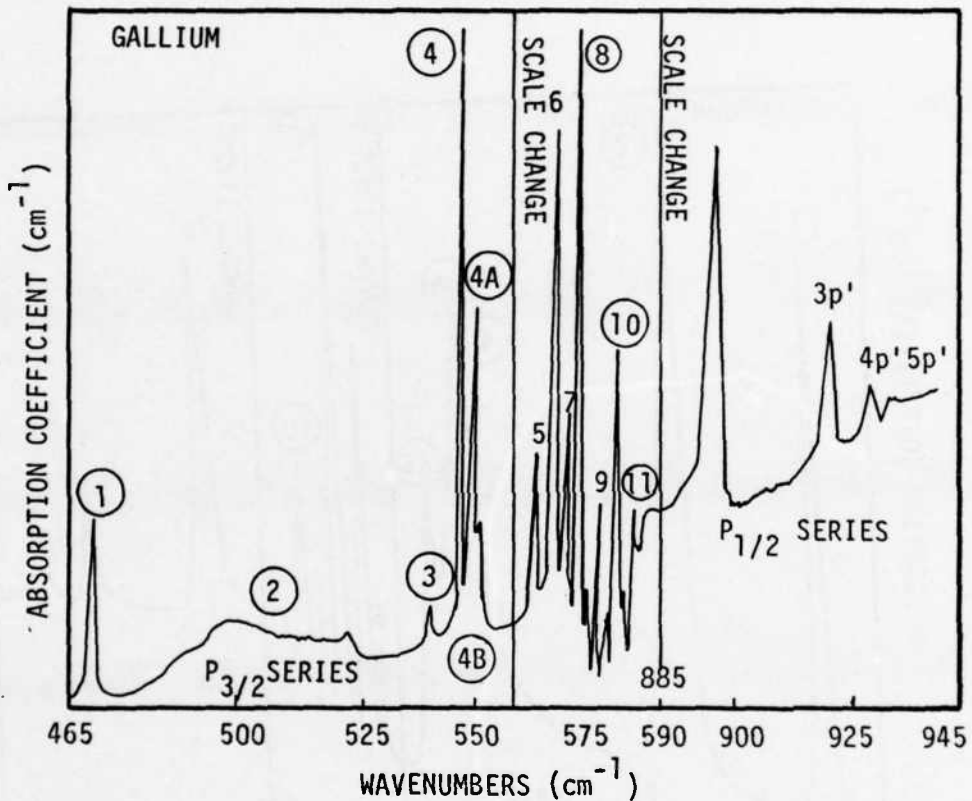


Figure 9. IR Absorption Spectrum of Gallium-Doped Silicon

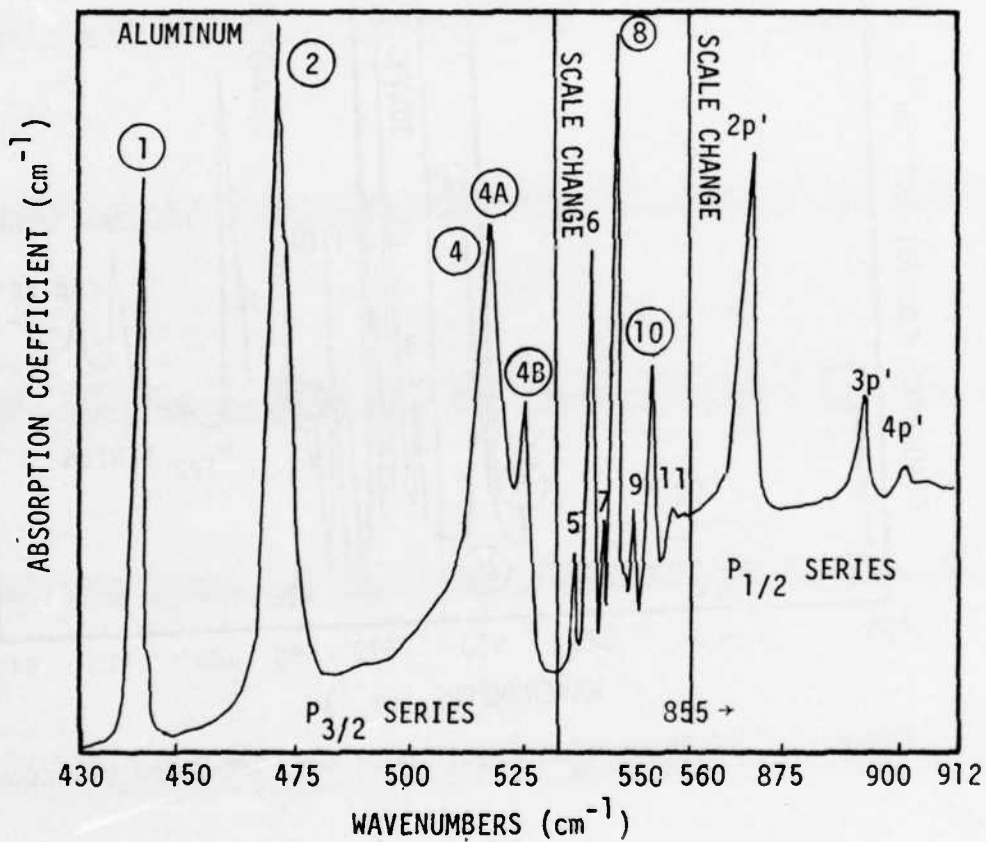


Figure 10. IR Absorption Spectrum of Aluminum-Doped Silicon

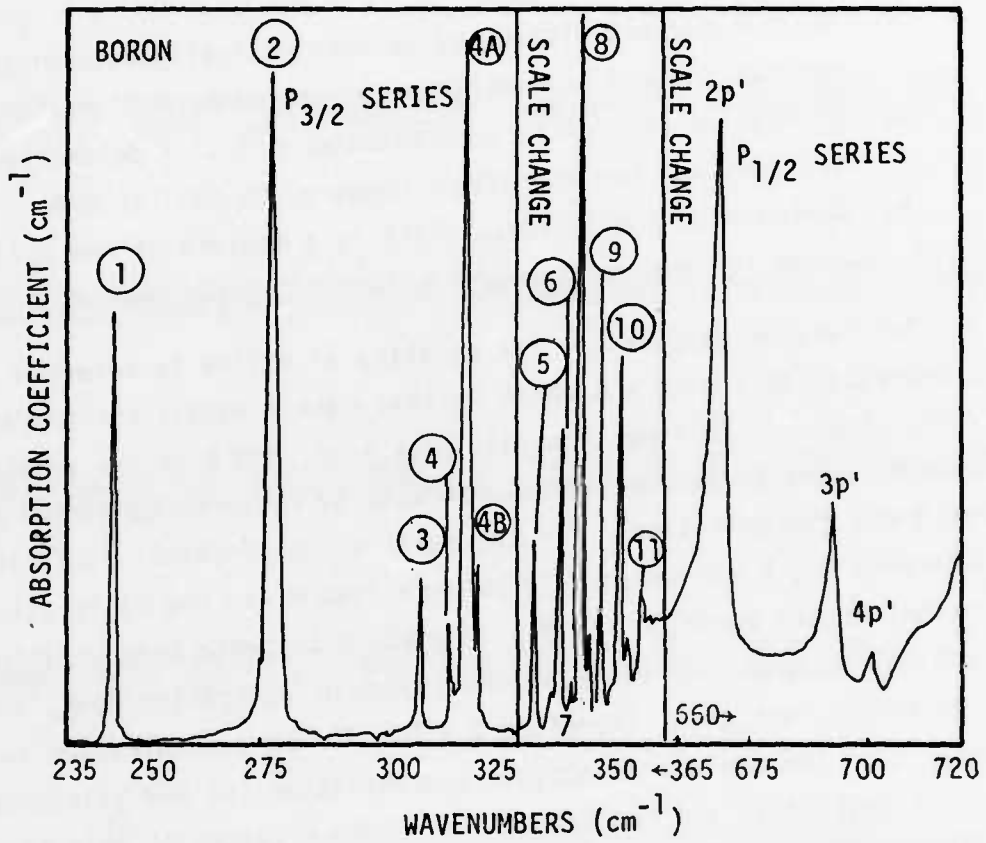


Figure 11. IR Absorption Spectrum of Boron-Doped Silicon

### 3. CALIBRATION RELATIONSHIPS

Experimentally determined calibration relationships are shown in Table 3, for the Group III acceptors indium, gallium, and boron. The other acceptor elements could not be done in this study. Thallium-doped samples were not available and concentration measurements on an aluminum-doped sample were not obtained. Some additional information also included in Table 3:

- a. Maximum percent difference between optically determined concentrations and concentrations measured by Hall or NAA.
- b. Average percent difference between optically determined concentrations and concentrations measured by Hall or NAA.
- c. Correlation coefficient, which is a measure of how well peak areas fit the particular function of concentration.

For further discussion, the equation of a line is referred to and is expressed as  $Y = MX + B$  where in this case  $Y$  equals concentration,  $M$  is the slope of the line,  $X$  equals peak area, and  $B$  is the  $y$ -intercept. Since  $B$  occurs at zero peak area, it will be referred to as the minimum detectable concentration. For the calibration constants in Table 1 (Reference 4),  $B$  was assumed to be zero, and  $M$  was the calibration constant in the equation  $Y = MX$ . Minimum detectable concentrations of Group III acceptors in silicon, using absorption spectroscopy, are known to be finite, not zero; therefore  $B \neq 0$ . If the concentration is much larger than the minimum detectable concentration ( $B$ ) the  $y$ -intercept term is negligible and can be ignored. Data obtained in this study shows that the  $y$ -intercept term is significant and must be included in any peak area versus concentration relationships. For example, it seems that indium line 2, shown in Figure 12a, behaves linearly with concentration. An attempt was made to use the slope of this line along with the  $y$ -intercept to form a relationship of peak area to concentration. This linear relationship was inadequate for use with small peak areas, resulting in negative concentrations. A markedly improved correlation over the linear case was obtained for the relationship between peak area and concentration<sup>1/3</sup> as shown in Figure 12b.

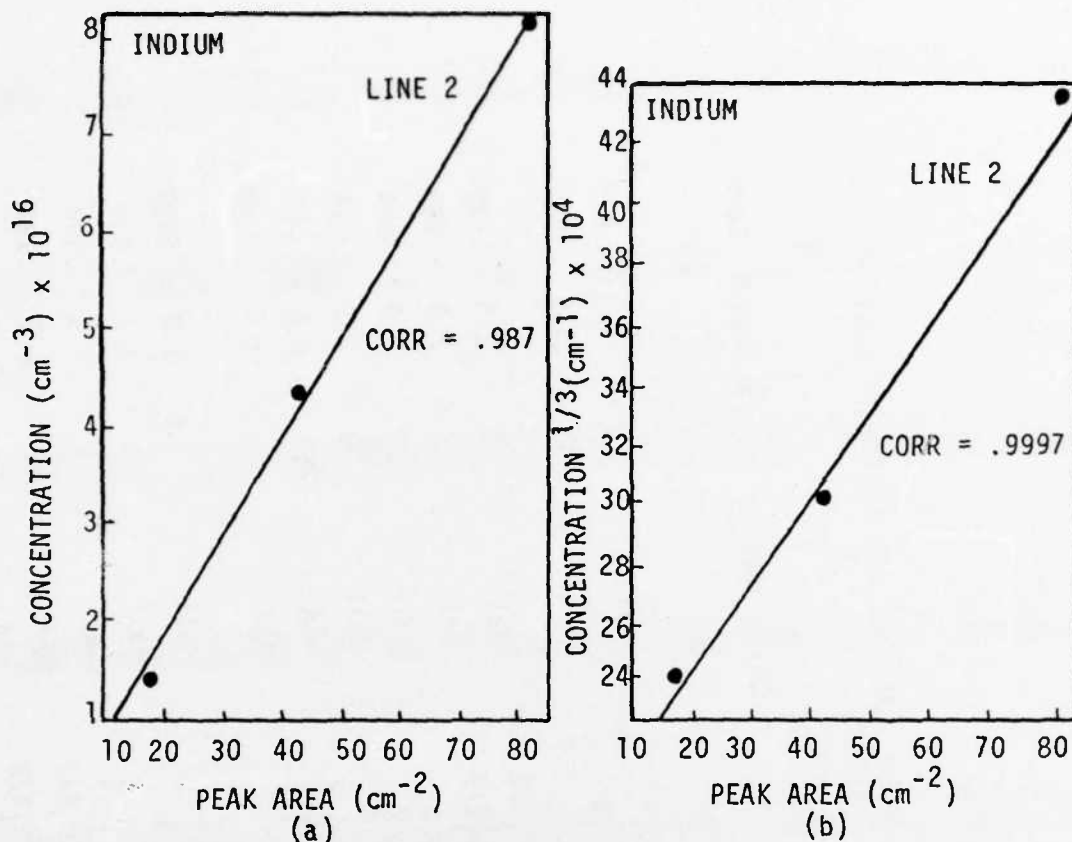


Figure 12. Indium Line 2 Peak Area Versus (a) Concentration, and (b) Concentration<sup>1/3</sup>

Because of the inadequacies of a simple linear relationship of peak area to concentration and because experimental evidence showed that such a linear relationship did not exist for the acceptor lines, other functional dependences of peak area to concentration were tested. Successful linear fits of peak area to concentration<sup>1/3</sup> and concentration<sup>2/3</sup> were made. The success of these fits was measured by the correlation coefficient obtained in a least-squares fit of peak area versus concentration<sup>1/3</sup> or concentration<sup>2/3</sup> data. The correlation coefficient of points forming a line is  $\pm 1$ . Correlation coefficients obtained for these fits ranged between .99 and .9999. The new calibration relationships which successfully relate peak area to concentration can be written in equation form as  $y^{1/3} = MX + B$  and  $y^{2/3} = MX + B$ . From a least-squares fit, a slope and y-intercept were computed. These equations along with their appropriate M and B values are shown in Table 3 and can be used with optical data to determine impurity concentrations.

TABLE 3

OPTICAL CALIBRATION RELATIONSHIPS FOR BORON, GALLIUM, AND INDIUM IN SILICON  
A = PEAK AREA

Line	Temp. Kelvin	Concentration ( $\text{cm}^{-3}$ )	Calibrated to	Max %	Ave %	Corr.
Boron						
3	5.5 - 8	$(A \times 5.28 \times 10^3 + 7.55 \times 10^4)^3$	Ha11	7	4.8	.995
2p'	5.5 - 8	$(A \times 2.83 \times 10^3 + 7.84 \times 10^4)^3$	Ha11	19	10.5	.99
Gallium						
1	5	$(A \times 7.03 \times 10^8 + 5.40 \times 10^9)^{3/2}$	Ha11	5	2.5	.9999
2p'	5 - 9	$(A \times 1.75 \times 10^9 + 4.21 \times 10^9)^{3/2}$	Ha11	16.6	7.9	.999
3p'	5	$(A \times 4.48 \times 10^4 + 8.44 \times 10^4)^3$	Ha11	10	7.0	.999
3	5	$(A \times 1.34 \times 10^4 + 8.53 \times 10^4)^3$	Ha11	10	7.3	.999
1	5 - 9	$(A \times 9.12 \times 10^8 + 8.52 \times 10^9)^{3.2}$	NAA	19	9.0	.999
2p'	5	$(A \times 2.27 \times 10^9 + 6.87 \times 10^9)^{3/2}$	NAA	5	3	.9998
Indium						
2	5	$(A \times 2.95 \times 10^3 + 1.92 \times 10^5)^3$	Ha11	2.6	1.8	.9997
2p'	5	$(A \times 4.69 \times 10^4 + 1.73 \times 10^5)^3$	Ha11	4	3.3	.999
2	5 - 9	$(A \times 1.48 \times 10^9 + 2.88 \times 10^{10})^{3/2}$	NAA	6	3.3	.999
2p'	5	$(A \times 2.35 \times 10^{10} + 1.98 \times 10^{10})^{3/2}$	NAA	2	1.3	.9997
3	5	$(A \times 2.63 \times 10^{10} + 3.72 \times 10^{10})^{3/2}$	NAA	19	11.7	.99

Data obtained in this study clearly shows that acceptor-line peak areas do not behave linearly with concentration. (Figures 12a, 13a, 14a, 15a, and 16a). Even though lines 2 and 3 of indium seem to behave linearly with concentration, a better correlation coefficient is obtained when these lines are plotted against concentration<sup>1/3</sup> (Figures 12b, 13b).

Previously reported optical calibration constants (Reference 4) assumed a linear relationship between peak area and acceptor concentration. The present work, however, shows that a simple linear relationship is inadequate for accurate measurements. New functional dependences were found which accurately relate peak area to concentration.

Notable and consistent differences in the concentration values reported by Hall analysis and neutron activation analysis on the same material were observed. This suggests a fundamental difference in what these techniques are measuring or how they are calibrated. Table 4 lists comparisons of the concentrations measured by the two techniques. Because of this difference between Hall and NAA, separate optical calibration relationships were determined to relate peak area to either Hall or NAA determined concentrations.

Slight changes in sample temperature caused measurable changes in peak area as noted in Section IV and shown in Figure 3. The usable temperature ranges of each calibrated acceptor line are listed in Table 3. These calibration relationships have not been tested for absorption data taken with sample temperatures higher than 9<sup>0</sup>K. Sample temperatures were measured using a silicon diode sensor attached to the copper sample holder. The temperature readout of these sensors was verified by observing the relative peak heights of the oxygen lines at 1136 cm<sup>-1</sup> and 1128 cm<sup>-1</sup> and using an oxygen thermometry curve developed in this study.

The oxygen lines at 1136 cm<sup>-1</sup> and 1128 cm<sup>-1</sup> were measured by absorption spectroscopy between 9 and 77<sup>0</sup>K. From these measurements, a thermometry curve was obtained which relates relative heights to sample temperature. This curve was useful for checking sample temperatures in both low oxygen content float-zoned material and high oxygen content Czochralski material. This curve is shown in Figure 8. By inspecting the oxygen lines in the resulting sample spectra and comparing the



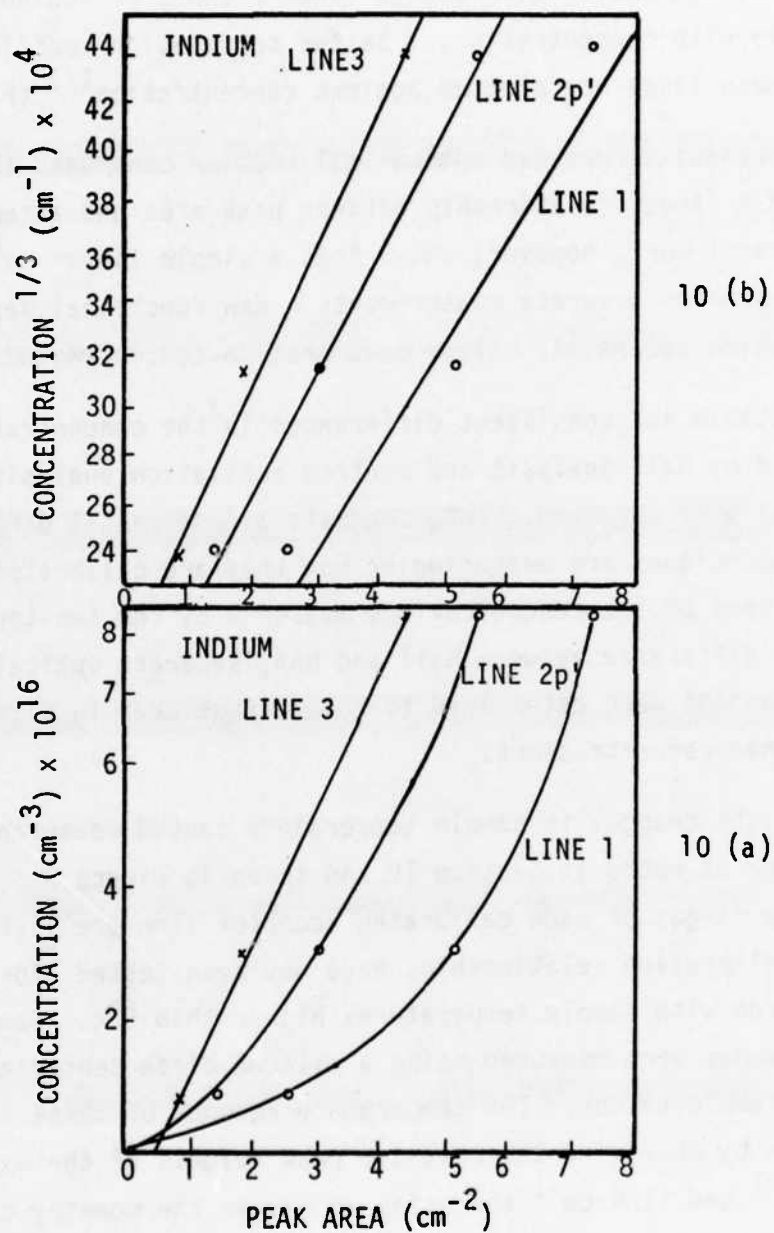


Figure 13. Indium Lines 1,3, and 2p' Peak Area Versus (a) Concentration and (b) Concentration<sup>1/3</sup>

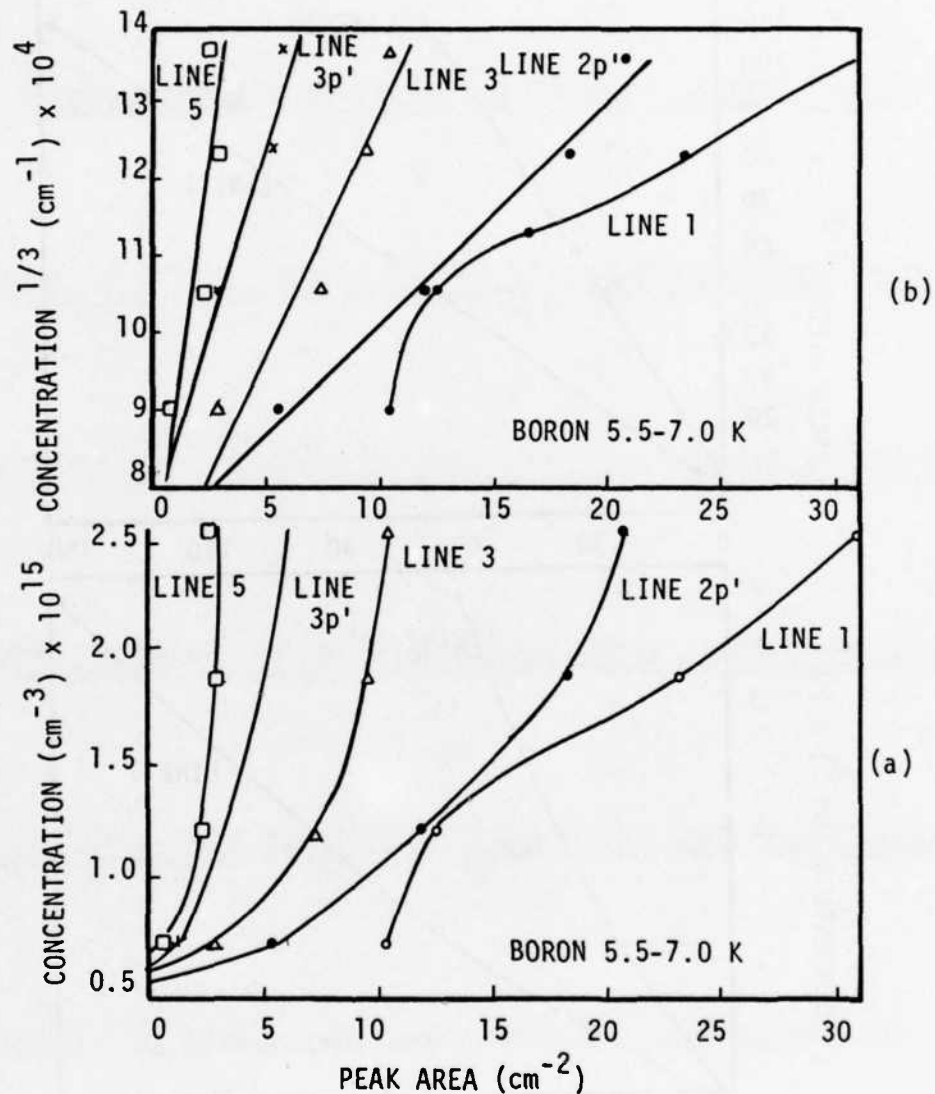


Figure 14. Boron Lines 1,3,5,2p', and 3p' Peak Area Versus  
 (a) Concentration and (b) Concentration<sup>1/3</sup>

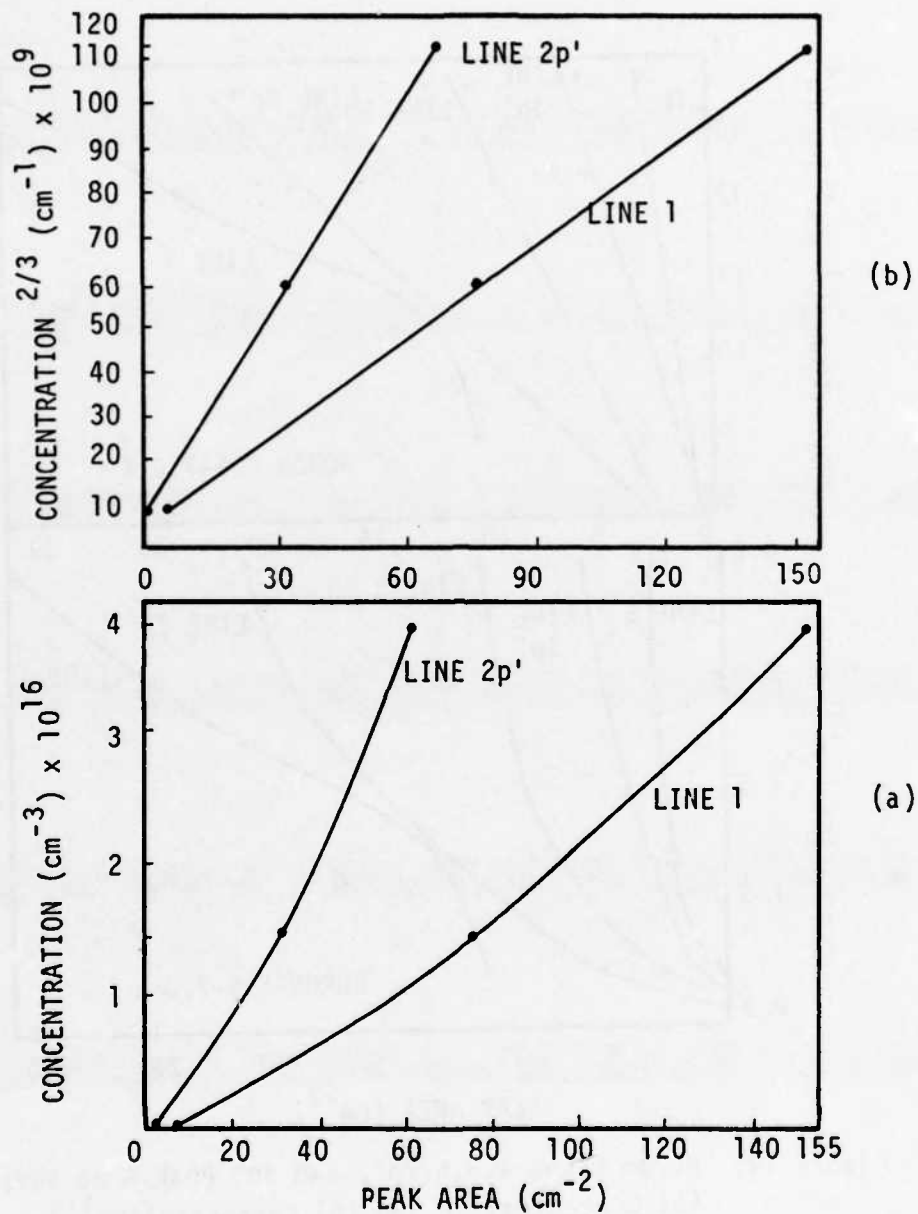


Figure 15. Gallium Lines 1 and 2p' Peak Area Versus  
 (a) Concentration and (b) Concentration<sup>2/3</sup>

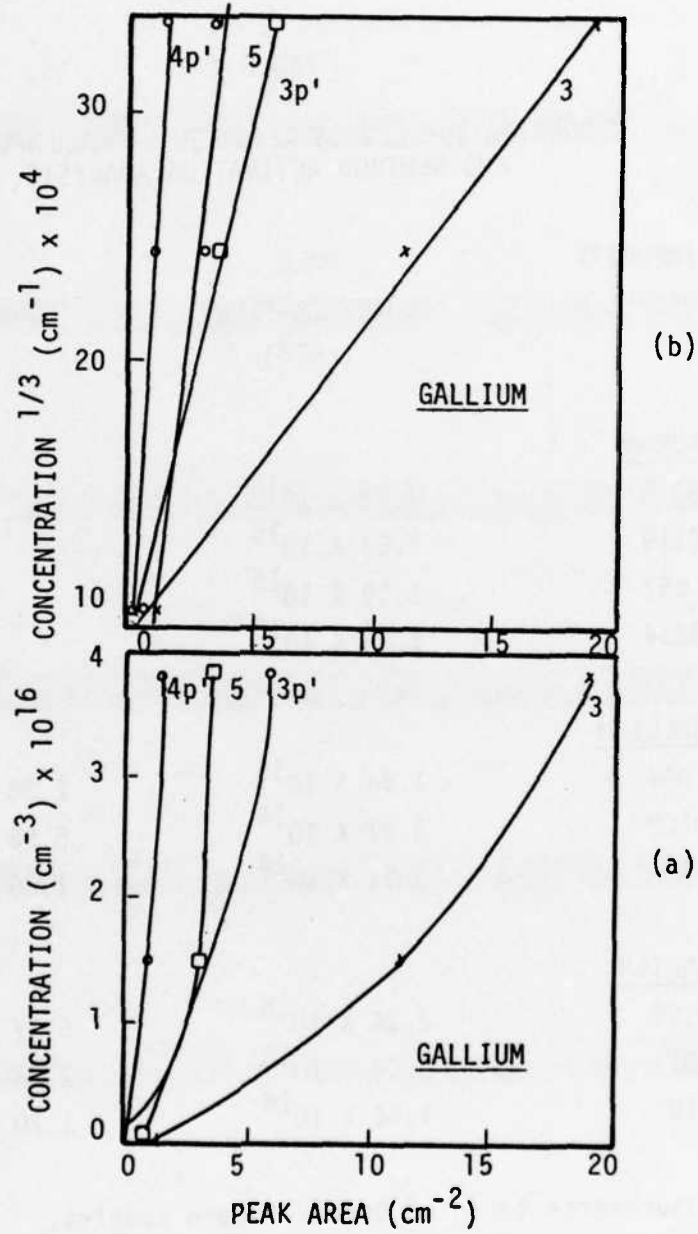


Figure 16. Gallium Lines 3,5,3p' and 4p', Peak Area Versus  
 (a) Concentration and (b) Concentration<sup>1/3</sup>

TABLE 4  
 CONCENTRATION LEVELS REPORTED BY HALL ANALYSIS  
 AND NEUTRON ACTIVATION ANALYSIS

IMPURITY SAMPLE #	HALL CONCENTRATION ( $\text{cm}^{-3}$ )	NAA CONCENTRATION ( $\text{cm}^{-3}$ )
<u>BORON</u>		
0118	$7.23 \times 10^{14}$	--*
0119	$2.53 \times 10^{15}$	--
657	$1.19 \times 10^{15}$	--
0234	$1.85 \times 10^{15}$	--
<u>GALLIUM</u>		
044	$1.44 \times 10^{16}$	$2.38 \times 10^{16}$
0102	$3.97 \times 10^{16}$	$5.56 \times 10^{16}$
987	$8.91 \times 10^{14}$	$1.26 \times 10^{15}$
<u>INDIUM</u>		
0109	$8.24 \times 10^{16}$	$5.77 \times 10^{16}$
011	$3.08 \times 10^{16}$	$2.86 \times 10^{16}$
0103	$1.44 \times 10^{16}$	$1.20 \times 10^{16}$

\* No NAA measurements taken on Boron - doped samples.

relative peak heights to the curve in Figure 8, one can estimate the actual sample temperature. If the sample has poor thermal contact to the copper cold tip, the sample temperature will be different from the temperature measured by the silicon-diode. Without this thermometry curve, any difference between sample and sample holder temperatures will not be detected. The results of this temperature study on the oxygen lines agree closely with those of Krishnan (Reference 2). Krishnan shows temperature dependence of each individual oxygen line in absorbance units. In this study, the relative peak heights of the two oxygen lines are related to sample temperature.

The tested concentration ranges of the new calibration relationships are unfortunately somewhat narrow due to limited sample availability. The concentration ranges for which these calibration relationships have been tested are:

	Low	High
Boron	$7.2 \times 10^{14} \text{ cm}^{-3}$	$2.5 \times 10^{15} \text{ cm}^{-3}$
Gallium	$3.6 \times 10^{14} \text{ cm}^{-3}$	$5.6 \times 10^{16} \text{ cm}^{-3}$
Indium	$1.2 \times 10^{16} \text{ cm}^{-3}$	$5.8 \times 10^{16} \text{ cm}^{-3}$

Without further testing, the applicability of these calibration relationships to concentrations outside these ranges can only be assumed.

A silicon sample containing measurable concentrations of indium, aluminum, aluminum-X, and boron was analyzed by the three techniques. The optical calibration relationships do not accurately relate concentrations measured by Hall and NAA, to peak areas measured by absorption spectroscopy, for this multiply-doped sample. Therefore, the use of these new calibration relationships in multiply-doped silicon samples may not produce accurate impurity concentrations.

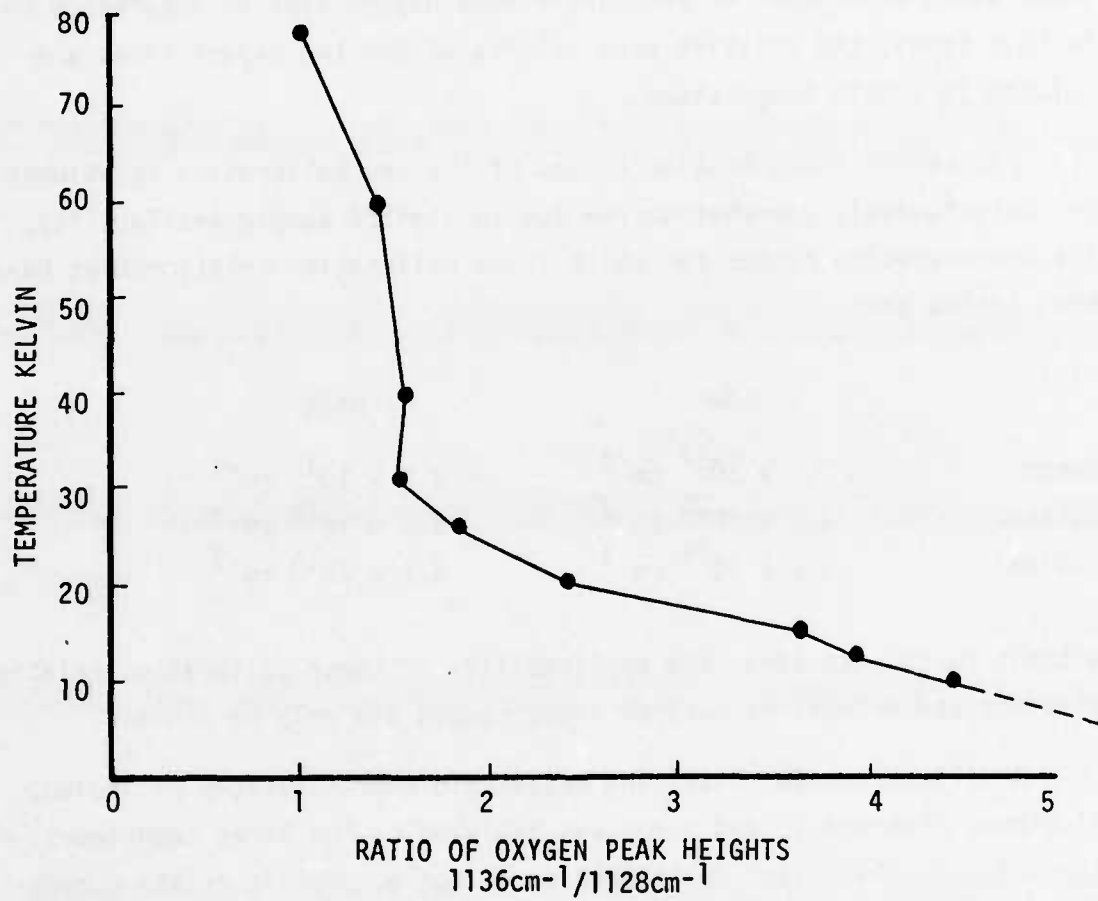


Figure 17. Oxygen Thermometry Curve



## SECTION V

## CONCLUSIONS AND RECOMMENDATIONS

The Group III acceptors indium, gallium, aluminum, and boron in silicon were studied using Fourier transform infrared absorption spectroscopy, variable-temperature Hall-effect analysis, and neutron activation analysis (NAA). From these measurements, new optical calibration relationships for In, Ga, and B were obtained, which relate acceptor peak area to impurity concentrations. Because neither Hall nor NAA measurements were made on Al-doped silicon, calibration relationships for Al were not obtained. Previously reported calibration constants (Reference 4) assumed a linear relationship between peak area and acceptor concentration. In the present work, a simple linear relationship is shown to be inadequate. New functional dependences have been found which accurately relate peak area to concentration. Significant and consistent differences in the concentration values reported by Hall and NAA required separate calibration relationships to relate a peak area to the concentration determined by either technique. The new calibration relationships have been tested for various sample temperatures and the temperature limitations are listed in Table 3. Sample temperatures indicated by the silicon diode sensors could be verified using the oxygen thermometry curve developed in this study and shown in Figure 8. The use of the new calibration relationships with samples containing more than one Group III impurity was unsuccessful, resulting in impurity concentrations significantly different than those measured by Hall or NAA.

Although the new calibration relationships accurately relate peak area to impurity concentration, additional studies can be made to extend their capabilities. These calibration relationships were obtained for somewhat narrow ranges of impurity concentration. Therefore, additional Hall, NAA, and FTIR measurements should be made on samples containing concentration outside the ranges included in this report. Also measurements on Al and Tl should be included to complete the optical capability to quantitatively measure all Group III impurities in silicon.

A considerable amount of research has been done to determine the relationship of acceptor peak halfwidth  $w_{1/2}$  to concentration, temperature,

compensation, etc. (References 5, 13, 16, 17) but little has been done to study the effects of these mechanisms on the entire peak area. This information could be used to further increase the capability to make accurate optical impurity concentration measurements.

Finally, a theoretical explanation for the particular functional dependence of peak area along with an explanation for the unsuccessful use of the calibration relationships with multiply-doped samples would be an appropriate answer to problems left unsolved in this work.

## APPENDIX

ADDITIONAL STRUCTURE IN INFRARED EXCITATION SPECTRA  
OF GROUP III ACCEPTORS IN SILICON

High resolution infrared  $p_{3/2}$  and  $p_{1/2}$  excitation spectra are reported for the Group III acceptors boron, aluminum, gallium, and indium in silicon. New lines are observed in the  $p_{3/2}$  spectra which are believed due to previously unresolved excited states. A  $5p'$  line is observed for the first time in the gallium spectrum. Some previously reported boron  $p_{3/2}$  lines are re-labeled to correspond with the other Group III spectra. A feature in each of the  $p_{3/2}$  spectra is defined as  $E_I$ , the ground state binding energy. Values measured for  $E_I$  are 44.39, 69.03, 72.73, and  $155.58 \pm 0.02$  meV for B, Al, Ga, and In, respectively. The data shows more complete correspondence of all the Group III excited state lines than any published previously. The spin-orbit splitting of the valence bands is measured to be  $44.00 \pm 0.02$  meV.

PACS numbers: 71.55Fr, 78.50Ge, 71.70Ej

## I. INTRODUCTION

Infrared excitation spectra of Group III acceptors in silicon have been reported previously by many different investigators. The reader is directed to a few of the more recent articles in which most of the previous data is referenced (References 4, 21, 22, 28, 29). In addition, several theoretical models have been proposed to interpret the experimental results. One of the more successful of these models appears to be the effective-mass theory of Lipari et al (References 11, 30). Despite the rather large number of papers published in this area, there are still some unsettled issues. Two examples are the accurate determination of ground state binding energies (Reference 11) and spin-orbit splitting of the valence bands. Furthermore, recently improved experimental techniques (primarily due to more widespread use of Fourier transform spectrometers) and improved growth techniques for doped silicon crystals have resulted in detailed high resolution data unobtainable by earlier workers.

We present here high resolution infrared absorption spectra for the Group III acceptors boron, aluminum, gallium, and indium in silicon. New lines and structure, unreported by previous investigators, are observed in the spectra. It is shown that the identity of some of the previously reported boron lines must be altered to be consistent with the other Group III spectra. It is demonstrated that a feature of the high energy side of peak 11 in each of the  $p_{3/2}$  spectra can be logically defined as  $E_I$ , the ground state binding energy. An analysis of this new data yields values for  $E_I$  and the spin-orbit splitting of the valence bands which are more consistent for all four acceptors than any of the previously reported values. A more complete correspondence of all the Group III excited state lines is also demonstrated.

## II. EXPERIMENTAL

Many different samples from a variety of sources were studied during the course of this work. The specific samples used to obtain the spectra illustrated in this report are as follows: the boron-doped sample was cut from a float-zone boule grown by Shin-Etsu Hondotai of Japan. It had a boron concentration of approximately  $2 \times 10^{15} \text{ cm}^{-3}$ . The aluminum-doped sample came from a float-zone crystal grown by Texas Instruments. It had an aluminum concentration of approximately  $5 \times 10^{15} \text{ cm}^{-3}$ . The gallium-doped sample was cut from a float-zone boule grown by Spectralab Inc. It had a gallium concentration of approximately  $1 \times 10^{15} \text{ cm}^{-3}$ . The indium-doped sample was cut from float-zone boule grown by Westinghouse. It had an indium concentration of approximately  $3 \times 10^{16} \text{ cm}^{-3}$ .

The samples were cooled to 5.5<sup>0</sup>K in a liquid helium dewar during measurement. All spectra were recorded on a Digilab model FTS-20C Fourier transform spectrophotometer at resolutions of 0.2 to 0.5  $\text{cm}^{-1}$ , with signal averaging of 1000 to 2000 scans. The spectrometer was calibrated using an internal laser reference line ( $6328\overset{0}{\text{Å}}$  HeNe laser at  $15800.8235 \text{ cm}^{-1}$  in vacuo) and also known position of water vapor and carbon dioxide absorption bands. A computer software program supplied with the Digilab system was used to convert transmittance to absorption coefficient. Samples were mounted in a stress-free manner by attaching them to the dewar cold finger by a very small dab of conducting vacuum grease at one corner only.

## III. RESULTS AND DISCUSSION

We obtained the excitation lines of both the  $p_{1/2}$  and  $p_{3/2}$  series by infrared absorption spectroscopy for each of the Group III acceptors boron, aluminum, gallium, and indium. In order to compare the spectra with each other on a common relative energy scale and to make a meaningful evaluation of the results, it was necessary to find an accurate reference point on which each spectrum could be aligned. Ideally, this reference point should be a spectral feature which exhibits no chemical shift or other meaningful change in relation to the intrinsic silicon band structure when the identity of the dopant acceptor is changed. In theory, the valence band edge should make an excellent reference point but no spectral features have been found to correspond to either the  $p_{3/2}$  band edge or to the split-off  $p_{1/2}$  band edge by previous workers. However, as demonstrated by Zwerdling et al (Reference 31), the  $p_{1/2}$  band edge can be determined from a Rydberg series plot of the  $p_{1/2}$  series absorption lines. The  $p_{1/2}$  series limit obtained from such a plot is assumed to be coincident with the band edge. The  $p_{1/2}$  series absorption spectra which we have obtained for the Group III acceptors in silicon are shown in Figure A-1.

The series limit,  $E_I^*$ , was determined for each spectrum by making a corrected Rydberg series plot in accordance with Zwerdling et al (Reference 31). The resultant  $E_I^*$  positions are indicated in Figure A-1, and it is these positions which were used to align the spectra with each other and which serve as the zero energy reference point. The actual values of  $E_I^*$  are listed in Table A-1. Zwerdling et al (Reference 31) plotted only the data for boron and found that both the corrected and uncorrected Rydberg series extrapolated to the same series limit. Since then, several other investigators have made the same assumption and have used the simple uncorrected series to determine the series limit (Reference 21). We find, however, that our data does not yield the same series limit for the corrected and uncorrected plots. In all cases, the corrected series limit is higher than the uncorrected one. The difference is 0.04 meV for B and In, 0.06 meV for Al, and 0.08 meV for Ga. Energy values of the absorption lines used to make the plots are given at the bottom of Table A-2. Notice that a  $5p'$  line is observed in the

gallium spectrum. This is the first time that a  $5p'$  line has been reported for any acceptor in silicon. It fits perfectly on the Rydberg series line and gives more confidence to the extrapolated series limit. Only three lines ( $2p'$ ,  $3p'$ , and  $4p'$ ) were observed in the B, Al, and In spectra.

Another feature to notice in both Figure A-1 and Table A-1 is that the energy separation between  $E_I^*$  and  $2p'$  is the same for all four acceptors. This is significant because it means that the  $2p'$  line is also an accurate reference point on which to align the spectra for comparison purposes. The importance of this is that  $2p'$  is an easily determined experimental position as opposed to the series limit which must be extrapolated. Onton et al (Reference 21) also used the  $2p'$  line as a reference point but their measured  $E_I^*-2p'$  separations were not the same, particularly in the case of indium. Our data, then, shows a consistency in the  $p_{1/2}$  spectra which previously reported data on the Group III acceptors in silicon did not show. The  $2p'$  line is also used as the reference point for comparing the  $p_{3/2}$  spectra which will be discussed next.

An example of a complete  $p_{3/2}$  absorption spectrum is shown for gallium in Figure A-2. Our spectrum is very similar to that shown by Chandrasekhar et al (Reference 22). The main difference is that our data exhibits a little better resolution and more detail in the high energy group of lines, i.e., lines numbered 5 and higher. Our other Group III  $p_{3/2}$  spectra also agree very well with previously published spectra for lines 1 through 4. It is in lines 5 and above where we observe some differences and on which we now direct the discussion. The high energy portion of the  $p_{3/2}$  spectra which we have obtained for B, Al, Ga, and In are shown in Figure A-3. These spectra are aligned with each other using the  $2p'$  line as the reference point. Previous investigators (References 21, 29, 32) had identified a total of six lines in this region, labeled 5, 6, 7, 8, 9, and 10 after notation first used by Colbow (Reference 14). Our spectra in Figure A-3 exhibit these six lines very clearly; more clearly, in fact than previous results. The major feature of our spectra is that several additional distinct lines and shoulders are also observed, particularly in the boron and gallium spectra.



It was considered prudent not to confuse matters by re-labeling the major lines (except for boron as will be discussed shortly) and so the new additional lines were labeled by using letter suffixes (A, B, C, etc.). New lines and shoulders which appear to be associated with the major line 10, for instance, are labeled 10A, 10B, 10C, and 10D as seen in Figure A-3. Also notice that a very distinct line 11 is observed in each spectrum for the first time. All previous data had indicated that line 10 was the highest energy line. The energy positions of all the lines are listed in Table A-2. Some of the new lines are observed in the spectra of all four acceptors but others occur only in some spectra and are missing in others. The line labels are consistent from one acceptor to another, however, because they were chosen on the basis of corresponding line positions as will be illustrated more clearly later in Figure A-5. Our values for the previously reported main lines are in good agreement with those of Onton et al (Reference 21). For completeness, the known line positions of thallium, which is also a Group III acceptor in silicon, are included in Table A-2. We were unable to obtain a good thallium-doped crystal and have therefore used the data of Scott and Schmit (Reference 33).

The first acceptor for which we observed this additional structure was boron. Our initial thought was that there was something peculiar about the sample or that some experimental problem such as external stress was the cause of this structure. We first satisfied ourselves that the sample was stress-free and then obtained other boron-doped silicon samples which yielded the same results. In the meantime two papers appeared (References 19, 34) which reported boron spectra virtually identical to ours but the additional structure was not discussed in either paper. Subsequently, we observed similar additional structure in other Group III spectra. These extra lines are most evident in boron, least evident in indium. It is believed that the spectra illustrated in Figure A-3 are stress-free and that the additional structure is truly characteristic of the Group III impurity. High quality samples and the use of a high resolution Fourier transform spectrometer are probably the main reasons why we were able to observe this structure and many previous workers were not.



One aspect of the boron spectrum that deserves special mention is line labeling. In Figure A-3, note the major boron lines labeled 8, 9, and 10. In all previously reported work (References 14, 19, 21, 28, 34) these lines are labeled 7, 8, and 9. It is evident from the comparison in Figure A-3 and Table A-2 (and later in Figure A-5) that from the standpoint of both relative peak intensity and relative energy position the peak at 42.74 meV (previously labeled 7) should be re-labeled 8 to be consistent with the labels subsequently given the lines of the other Group III acceptors. This same argument applies to lines 9 and 10. Line 7 is actually the weak peak at 42.41 meV which is reported here for the first time. This new boron line 7 is also consistent with line 7 of the other Group III spectra in relative energy position and relative intensity. The line positions listed in Table A-2 include the re-labeled lines 7, 8, 9, and 10 of boron.

Another point to notice in Figure A-3 is the feature at the high energy end of each spectrum which is labeled  $E_I$ . This is the point which we are tentatively defining as the  $p_{32}$  valence band edge. By definition, the energy position of this point also represents the binding energy of the Group III acceptor ground state,  $E_I$ . The actual value of the ground state binding energies has been the subject of much previous discussion, both experimentally and theoretically (References 4, 11, 21, 28, 30). One of the problems in determining an accurate value for  $E_I$  is that in previous experimental work no spectral feature could be identified as corresponding to the band edge. In our spectra, there is a reproducible minimum on the high energy side of line 11 beyond which there is a more or less flat featureless continuum absorption. That minimum falls at precisely the same relative energy position for each of the Group III acceptors. The rationale behind our suggestion that this spectral feature be defined as  $E_I$  is illustrated in Figure A-4.

Shown in Figure A-4 is an enlarged view of the boron spectrum from Figure A-3. One noticeable aspect of this spectrum is that the background immediately to the high energy side of line 11 is significantly higher than the background under the main lines and that it is relatively flat and featureless. The dashed curve represents our estimate of the

background position under the lines. It appears that the background gradually slopes upward as the energy increases toward the line 11 position. At the high energy side of line 11 there is a sudden break in the slope. We are suggesting that this break represents the onset of continuum absorption into the valence band. In other words, we are observing the valence band absorption edge which is logically the position of  $E_I$ . This same background break is also observed in the aluminum, gallium, and indium spectra. The energy value of this position is listed as  $E_I$  in Table A-2. The region around line 11, in fact, is very similar in appearance to some other semiconductor absorption edge spectra in which an exciton peak occurs immediately below the edge (Reference 35). The minimum on the high energy side of line 11, which corresponds to the break in the background slope, occurs at the same relative energy position for each of the impurities. This means that the energy separation between our measured  $E_I$  and  $E_I^*$  is constant for each acceptor.  $E_I^* - E_I$  is, by definition, the spin-orbit splitting of the valence bands. Our measured value, as listed in Table A-1, is  $44.00 \pm 0.02$  meV which is in good agreement with the values of Onton et al (Reference 21) and Zwerdling et al (Reference 31). The fact that we get the same value of  $E_I^* - E_I$  for each of the acceptors when the position of  $E_I$  is measured as described above is a strong point in support of our interpretation. No previously reported data shows such a consistent value for the spin-orbit splitting for all four of these Group III dopants in silicon.

Our measured values of  $E_I$ , the ground state binding energies, are compared with values reported by some other workers in Table A-3. We agree well with the experimental results of Jones et al (Reference 4) for B and Ga and less well for Al and In. There is not close agreement with the values of Lipari et al (Reference 11) and Ramdas et al (Reference 28). Lipari et al calculated the binding energies of some of the excited states for Group III acceptors in silicon. They calculated that the excited state giving rise to absorption line 6 had a binding energy of 3.67 meV and then added this energy to the experimental line 6 energy to come up with the ground state binding energy. Ramdas et al (Reference 28) added 6.1 meV to line 4 to obtain their ground state binding energy values. The problem with adding a given energy to an

experimental absorption line position in this case is that the lines tend to shift around in relative energy position from one acceptor to another. This is particularly true of line 4 as illustrated in Figure A-5 and as also shown in previous work (Reference 21).

Shown in Figure A-5 are the relative binding energy positions of the Group III excited states in silicon as determined from our infrared absorption spectra. Our measured value of  $E_I$  is used as the zero energy reference point for each acceptor. Positions for lines 1 and 2 are not shown because they are off scale to the top of the figure. The longer lines in Figure A-5 represent the major absorption peaks 3 through 11. Shorter lines represent new absorption structure 6A, 6B, 8A etc. as listed in Table A-2. Notice that lines 3, 4, and 5 exhibit significant chemical shifts. Lines 6 through 11, on the other hand, show good correspondence from one acceptor to another. Most of the new lines also show good correspondence. It was on the basis of such corresponding line positions, for instance, that the distinct new shoulders observed in the indium spectrum (Figure A-3) were labeled 8A, 10A, 10D, and 11B (Table A-2). In other words, all line labels listed in Table A-2 were chosen on the basis of corresponding line positions as seen in Figure A-5.

Chandrasekhar et al (Reference 22) have shown that the lack of a sharp line 2 in the gallium spectrum is due to a resonant interaction with optical phonons. The absence of line 3 in the aluminum spectrum is believed due to a similar interaction (References 21, 22). Line 4 of aluminum is also somewhat peculiar, however. As seen in Figure A-5, the relative energy positions of the line 4 components are significantly shifted with respect to the other Group III acceptors. In addition, aluminum line 4 has a strange shape and is much weaker in relation to the other spectral lines than the other three acceptors. We have observed a new line 4 component, labeled 4' in Table A-2. It is pointed out that the zone center optical phonon which causes the resonant interaction in line 2 of gallium (Reference 22) has an energy which falls between lines 4 and 4A in aluminum. Perhaps the strange behavior of aluminum line 4 is due to this phonon interference. At any rate, using line 4 to determine binding energies as done by Ramdas and Rodriguez (Reference 28) will yield doubtful results, especially for aluminum.

## IV. SUMMARY

We have presented the  $p_{1/2}$  and  $p_{3/2}$  infrared absorption spectra of the Group III acceptors boron, aluminum, gallium, and indium in silicon. At least ten new lines were observed in the  $p_{3/2}$  spectra. These new lines appear to represent additional excited states which had not been previously resolved. The previously reported identity of some of the boron  $p_{3/2}$  lines was changed to make them consistent with the other Group III spectra. A new  $5p'$  line was also observed for the first time in the  $p_{1/2}$  spectrum of gallium. Corrected Rydberg series plots were made from the  $p_{1/2}$  series lines and used to determine the series limit,  $E_I^*$ . The value of  $E_I^*$  was of interest because it seemed to be a logical reference point on which to base a relative energy scale comparison of the various spectra. It was shown that the  $2p'$  line is also an accurate reference point with the added advantage that it is easily seen experimentally. A feature on the high energy side of peak 11 in the  $p_{3/2}$  spectra was identified as  $E_I$ , the ground state binding energy. This identification was based on the behavior of the background in the region of the valence band edge and this position of  $E_I$  was found to be at the same relative energy position for each of the four acceptors. The specific values of  $E_I$  determined here were 44.39, 69.03, 72.73, and 155.58 meV for boron, aluminum, gallium, and indium, respectively. It was also shown that the experimentally determined spin-orbit splitting of the valence bands,  $E_I^* - E_I$ , was the same for each acceptor, the value being  $44.00 \pm 0.02$  meV. This was the first experimental data to show such a consistent  $E_I^* - E_I$  value for all four Group III acceptors in silicon. Other aspects of the data such as relative line positions also show excellent consistency from one acceptor to another. In fact, our relative line positions and intensities (after re-labeling some of the boron lines) are more consistent across the Group III series than any previously reported data.

The authors wish to thank Dr. T. Abe of Shin-Etsu Hondotai Co., Japan, for the boron doped crystal used in this investigation and Mr. Terry Trumble of the Aero Propulsion Laboratory (AFWAL/POOC) for the gallium-doped crystal grown by Spectralab Inc. under Contract No. F33615-80-C-2009. We also thank Robert Bertke of the University of Dayton

Research Institute for sample preparation and Drs. Melvin Ohmer and Patrick Hemenger of this Laboratory for helpful discussions and comments.

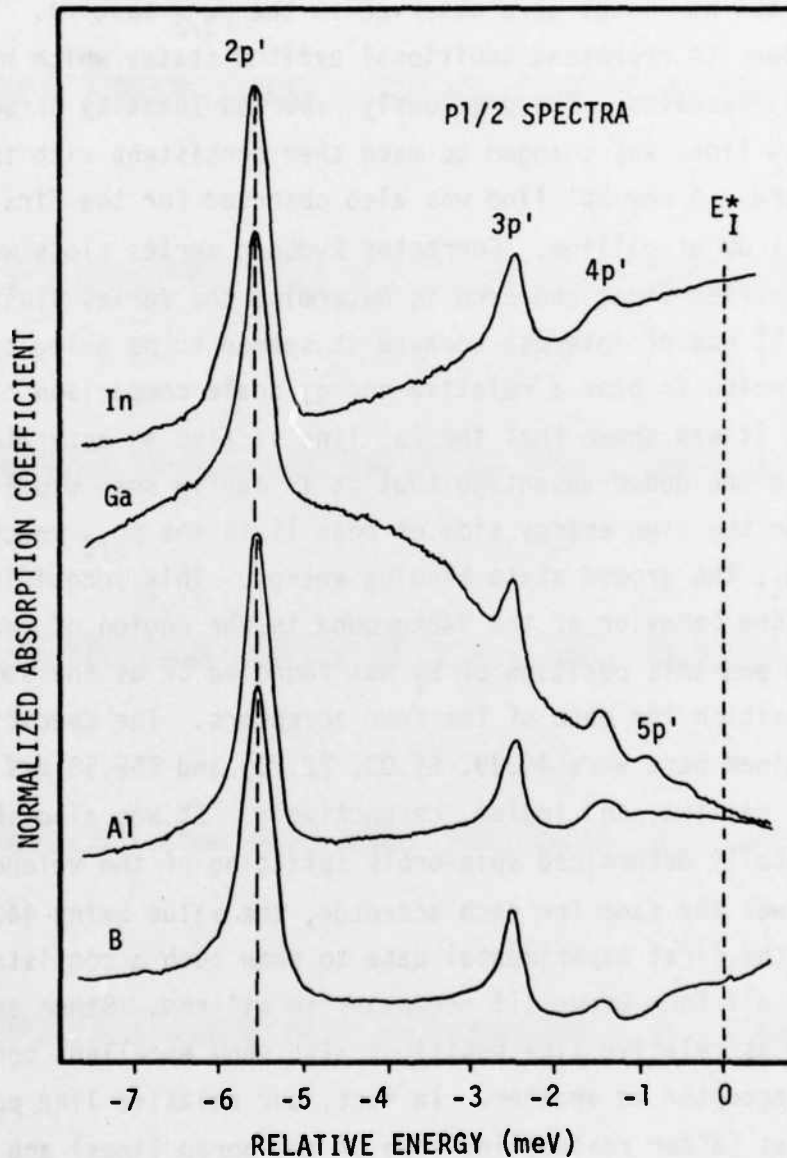


Figure A-1.  $p_{1/2}$  Series Absorption Spectra of Group III Acceptors in Silicon. (Spectra are aligned on  $E_I^*$ , the series limit, which is placed at zero energy for comparison purposes.  $E_I^*$  was determined from a corrected Rydberg series following Zwerdling et al (Reference 8). The  $2p'$  lines were normalized to same intensity for comparison.)

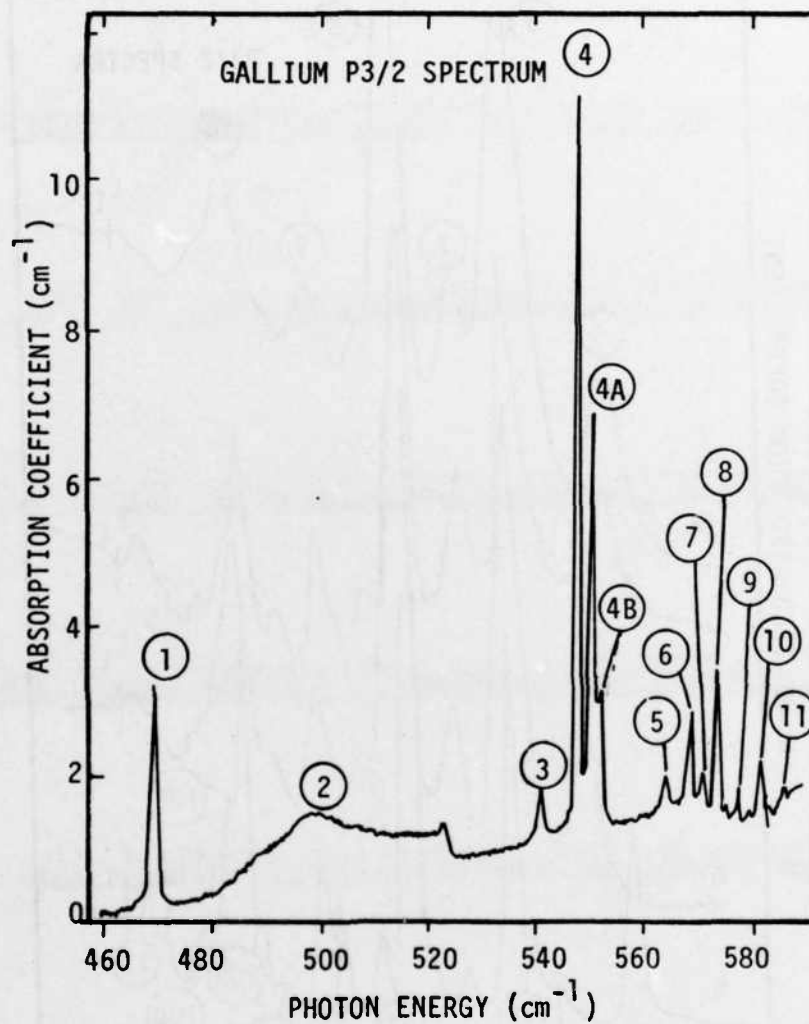


Figure A-2. p<sub>3/2</sub> Series. Absorption Spectrum of Gallium in Silicon. (Sample temperature was 5.5°K. Note detail in high energy group of lines labeled 5 through 11.)



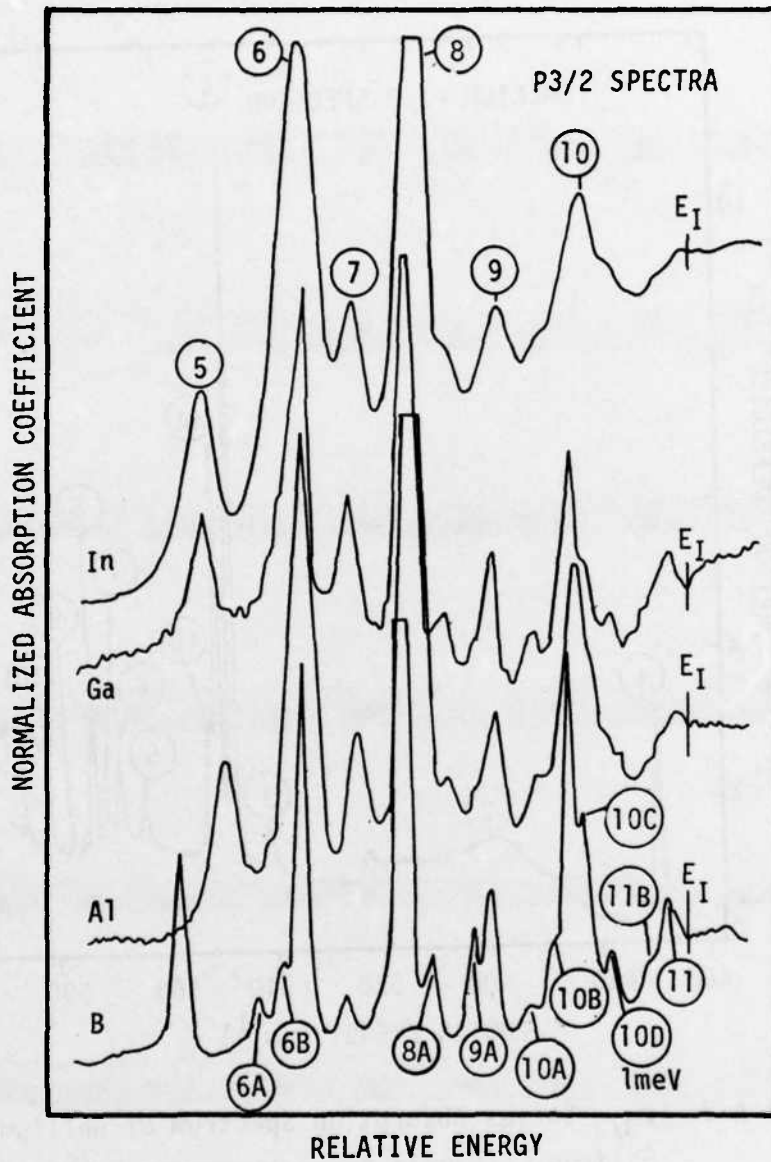


Figure A-3. High Energy Region of  $p_{3/2}$  Absorption Spectra of Group III Acceptors in Silicon. (Spectra are aligned using  $2p'$  line as reference. Rationale for labeling of peaks and band edge  $E_I$  are explained in text.)



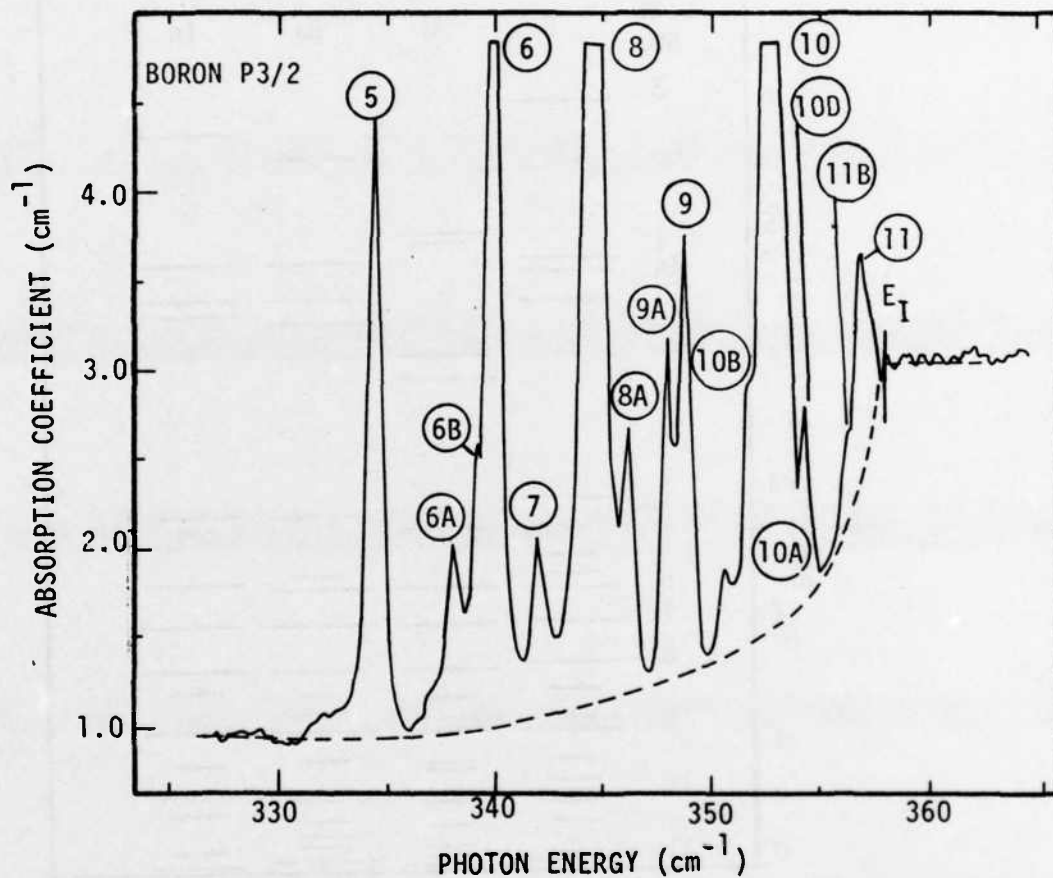


Figure A-4. High Energy Region of p<sub>3/2</sub> Absorption Spectrum of Boron in Silicon (Dashed curve is estimated background.)

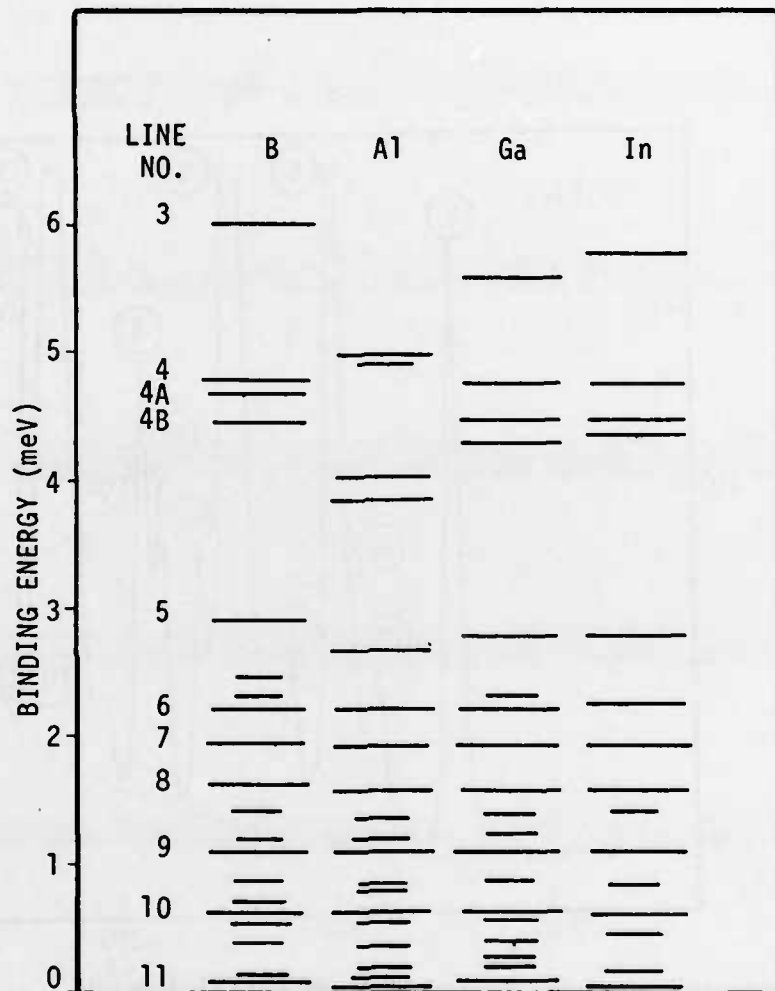


Figure A-5. Experimental Binding Energies of Excited States of Group III Acceptors in Silicon (Zero energy is placed at experimentally determined band edge,  $E_I$ . Longer lines represent major absorption peaks 3 through 11. Shorter lines represent new absorption structure 6A, 6B, 8A etc. as listed in Table A-2.)

TABLE A-1

$P_{1/2}$  SERIES IONIZATION ENERGY<sup>a</sup> AND SOME EXPERIMENTAL  
ENERGY SEPARATIONS IN SILICON (UNITS ARE meV<sup>b</sup>)

	<u>B</u>	<u>Al</u>	<u>Ga</u>	<u>In</u>
$E_I^*$	88.39	113.04	116.73	199.58
$E_I^* - 2p'$	5.50	5.51	5.49	5.50
$E_I^* - E_I$	44.00	44.01	44.00	44.01
$2p' - E_I$	38.50	38.50	38.51	38.51

<sup>a</sup> $E_I^*$  determined from corrected Rydberg Series given by Zwerdling et al (Reference 31).

<sup>b</sup>Maximum error estimated to be  $\pm 0.02$  meV.

TABLE A-2  
 EXPERIMENTAL ENERGY POSITIONS OF GROUP III ACCEPTOR  
 EXCITATION LINES IN SILICON (UNITS ARE meV<sup>a</sup>)

Line	Boron	Aluminum	Gallium	Indium	Thallium <sup>b</sup>
1	30.37	54.89	58.24	142.01	232.6
2	34.49	58.51	---	145.78	236.4
3	38.35	---	67.13	149.77	240.2
4	39.59	64.04(A) 64.12(B)	67.97	150.80	241.5
4A	39.67	64.98	68.26	151.08	
4B	39.91	65.16	68.44	151.19	
5	41.47	66.35	69.95	152.77	
6A	41.91	---	---	---	
6B	42.06	---	(70.40)	---	
6	42.16	66.79	70.51	153.31	244.0
7	42.41	67.10	70.79	153.62	
8	42.74	67.43	71.13	153.98	
8A	42.92	67.64	71.35	(154.15)	
9A	43.16	(67.81)	(71.53)	---	
9	43.24	67.91	71.62	154.46	
10A	43.49	68.16	71.85	(154.72)	
10B	(43.64)	(68.22)	---	---	
10	43.71	68.38	72.07	154.93	
10C	43.78	(68.53)	(72.13)	---	
10D	43.95	68.62	72.31	(155.08)	
11A	---	(68.80)	(72.44)	---	
11B	(44.20)	(68.87)	(72.52)	(155.40)	
11	44.27	68.96	72.62	155.51	
E <sub>I</sub>	44.39	69.03	72.73	155.57	246.2
2p'	82.89	107.53	111.24	194.08	283.3
3p'	85.90	110.56	114.25	197.11	286.3
4p'	86.95	111.61	115.30	198.18	
5p'	---	---	115.8	---	
E <sub>I</sub> <sup>*</sup>	88.39	113.04	116.73	199.58	

<sup>a</sup>Error is estimated to be  $\pm 0.02$  meV for all lines of B, Al, Ga, and In except those in parentheses where error is estimated to be  $\pm 0.05$  meV.

<sup>b</sup>Reference 33. Error estimate not given.

TABLE A-3

$P_{3/2}$  GROUND STATE IONIZATION ENERGIES OF GROUP III  
ACCEPTORS IN SILICON (UNITS ARE meV)

	<u>B</u>	<u>Al</u>	<u>Ga</u>	<u>In</u>
Lipari et al <sup>a</sup>	45.83	70.42	76.16	156.94
Ramdas et al <sup>b</sup>	45.71	70.18	74.05	156.90
Jones et al <sup>c</sup>	44.3	68.5	72.7	156.0
This work	44.39	69.03	72.73	155.58

<sup>a</sup>Reference 11

<sup>b</sup>Reference 28

<sup>c</sup>Reference 4

## REFERENCES

1. NMAB Report No. 362 Report of the Committee on the Preparation of UltraHigh-Purity, Low-Boron Silicon, A. F. Witt chairman, (National Academy Press, New York, 1981).
2. K. Krishnan, Digilab Brochure, Note No. 39, (1981).
3. N. Sclar, IEEE Trans. Electronic Devices ED-24, 709 (1977).
4. C. E. Jones, D. Schafer, W. Scott and R. J. Hager, J. Appl. Phys. 52, 5148 (1981).
5. S. C. Baber, Thin Solid Films 72, 210 (1980).
6. B. O. Kolbesen, Appl. Phys. Lett. 27, 353 (1975).
7. K. Krishnan, Digilab Brochure, Fourier Transform Infrared Spectroscopic Study of Oxygen Impurity in Silicon.
8. W. Kohn, Solid State Physics, edited by F. Seitz and D. Turnbull, 5, 257 (Academic, New York, 1957).
9. P. Fisher and A. K. Ramdas, Physics of Solid State, edited by S. Balakrishna, M. Krishnamurthi, and B. Ramachandra Rao, 149 (Academic, New York, 1969).
10. D. Schechter, J. Phys. Chem. Solids 23, 237 (1962).
11. N. O. Lipari, A. Baldereschi, and M. L. Thewalt, Solid State Commun. 33, 277 (1980).
12. W. R. Thurber, NBS Tech. Note 529, (1970).
13. J. J. White, Can. J. Phys. 45, 2797 (1967).
14. K. Colbow, Can. J. Phys. 41, 1801 (1963).
15. M. Lax and E. Burstein, Phys. Rev. 100, 592 (1955).
16. R. Newman, Phys. Rev. 103, 103 (1956).
17. J. J. White, Can. J. Phys. 45, 2695 (1967).
18. D. M. Larsen, Phys. Rev. B 13, 1681 (1976).
19. C. Jagannath, Z. W. Grabowski, and A. K. Ramdas, Phys. Rev. B 23, 2082 (1981).
20. G. A. Vannsaee editor, Spectrometric Techniques Vol.II (Acad. Press, New York, 1981).
21. A. Onton, P. Fisher, and A. K. Ramdas, Phys. Rev. 163, 686 (1967).

## REFERENCES (Concluded)

22. H. R. Chandrasekhar, A. K. Ramdas, and S. Rodriguez, *Phys. Rev. B* 14, 2417 (1976).
23. A. R. H. Cole ed., Tables of Wavenumbers for the Calibration of Infrared Spectrometers (Pergamon Press, New York, 1977).
24. L. J. van der Pauw, *Phil. Res. Rep.* 13, 1 (1958).
25. V. Swaninathan, J. E. Lang, P. M. Hemenger, and S. R. Smith, *Appl. Phys. Lett.* 35, 184 (1976).
26. F. L. Madarasz, J. E. Lang, and P. M. Hemenger, *J. Appl. Phys.* 52, 4646 (1981).
27. E. H. Putley, The Hall Effect in Semiconductor Physics Dover, New York, 1968).
28. A. K. Ramdas and S. Rodriguez, *Reports on Progress in Physics*, 44 (12), 1297 (1981).
29. J. J. Rome, R. J. Spry, T. C. Chandler, G. J. Brown, B. C. Covington and R. J. Harris, *Phys. Rev. B* 25, 3615 (1982).
30. N. O. Lipari and A. Baldereschi, *Solid State Commun.* 25, 665 (1978).
31. S. Zwerdling, K. J. Button, B. Lax and L. M. Roth, *Phys. Rev. Lett.* 4, 173 (1960).
32. B. C. Covington, R. J. Harris and R. J. Spry, *Phys. Rev. B* 22, 778 (1980).
33. W. Scott and J. L. Schmit, *Appl. Phys. Lett.* 33, 294 (1978).
34. B. Pajot and D. Debarre, Netwon - Transmutation Doped Silicon, edited by J. Guldberg (Plenum Press, New York, 1981).
35. R. J. Elliott, *Phys. Rev.* 108, 1384 (1957).
36. J. L. Pankove, Optical Processes in Semiconductors, (Dover Publications, New York, 1971).



**END**

**FILMED**

**12-83**

**DTIC**





DTIC